NASA/TP-1998-208463

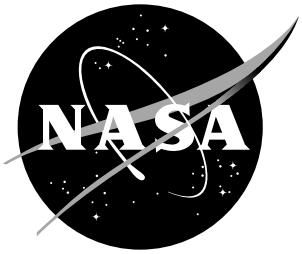

A Control Law Design Method Facilitating Control Power, Robustness, Agility, and Flying Qualities Tradeoffs: CRAFT

Patrick C. Murphy and John B. Davidson
Langley Research Center, Hampton, Virginia

September 1998

The NASA STI Program Office ... in Profile

Since its founding, NASA has been dedicated to the advancement of aeronautics and space science. The NASA Scientific and Technical Information (STI) Program Office plays a key part in helping NASA maintain this important role.

The NASA STI Program Office is operated by Langley Research Center, the lead center for NASA's scientific and technical information. The NASA STI Program Office provides access to the NASA STI Database, the largest collection of aeronautical and space science STI in the world. The Program Office is also NASA's institutional mechanism for disseminating the results of its research and development activities. These results are published by NASA in the NASA STI Report Series, which includes the following report types:

- TECHNICAL PUBLICATION. Reports of completed research or a major significant phase of research that present the results of NASA programs and include extensive data or theoretical analysis. Includes compilations of significant scientific and technical data and information deemed to be of continuing reference value. NASA counter-part of peer reviewed formal professional papers, but having less stringent limitations on manuscript length and extent of graphic presentations.

- TECHNICAL MEMORANDUM. Scientific and technical findings that are preliminary or of specialized interest, e.g., quick release reports, working papers, and bibliographies that contain minimal annotation. Does not contain extensive analysis.

- CONTRACTOR REPORT. Scientific and technical findings by NASA-sponsored contractors and grantees.

- CONFERENCE PUBLICATION. Collected papers from scientific and technical conferences, symposia, seminars, or other meetings sponsored or co-sponsored by NASA.

- SPECIAL PUBLICATION. Scientific, technical, or historical information from NASA programs, projects, and missions, often concerned with subjects having substantial public interest.

- TECHNICAL TRANSLATION. English-language translations of foreign scientific and technical material pertinent to NASA's mission.

Specialized services that help round out the STI Program Office's diverse offerings include creating custom thesauri, building customized databases, organizing and publishing research results ... even providing videos.

For more information about the NASA STI Program Office, see the following:

- Access the NASA STI Program Home Page at ***http://www.sti.nasa.gov***

- E-mail your question via the Internet to help@sti.nasa.gov

- Fax your question to the NASA Access Help Desk at (301) 621-0134

- Phone the NASA Access Help Desk at (301) 621-0390

- Write to:
  NASA Access Help Desk
  NASA Center for AeroSpace Information
  7121 Standard Drive
  Hanover, MD 21076-1320

NASA/TP-1998-208463

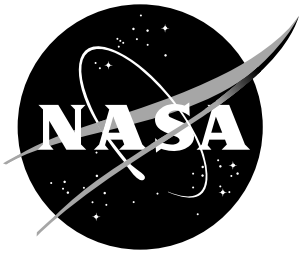

A Control Law Design Method Facilitating Control Power, Robustness, Agility, and Flying Qualities Tradeoffs: CRAFT

Patrick C. Murphy and John B. Davidson
Langley Research Center, Hampton, Virginia

National Aeronautics and
Space Administration

Langley Research Center
Hampton, Virginia 23681-2199

September 1998

Available from the following:

NASA Center for AeroSpace Information (CASI)
7121 Standard Drive
Hanover, MD 21076-1320
(301) 621-0390

National Technical Information Service (NTIS)
5285 Port Royal Road
Springfield, VA 22161-2171
(703) 487-4650

Summary

Recent advances in aircraft technology are placing increasing demands on flight control designers to satisfy many competing design objectives. Advances in weapons and aircraft technology are significantly changing air combat for the next generation of fighter aircraft. New control effectors, such as thrust vectoring, offer the capability to expand the flight envelope, but also complicate the control mix with redundant effectors. Future fighters will operate in environments where having high levels of maneuverability and controllability, throughout a greatly expanded flight envelope, are requirements. These diverse and often competing requirements have created a need for a design method that allows production of a balanced final design.

The control law design methodology outlined in this report enables a designer to integrate numerous design requirements into one design process. This methodology, known as CRAFT, is named for the design objectives addressed, namely, Control Power, Robustness, Agility, and Flying Qualities Tradeoffs. The approach combines eigenspace assignment with a graphical technique for representing numerous design goals in one composite illustration. The design goals are represented by control design metrics that are quantitative measures of specific system capabilities translating desired operational characteristics into useful engineering terms for control design. The methodology described in this report makes use of control design metrics from the four design objective areas indicated. Although these metrics are key in control law design for fighter aircraft, the methodology is more broadly applicable and any metric quantifying design requirements can be used; for example, metrics characterizing ride quality, weapons control, or structural requirements may be key in certain designs.

The CRAFT methodology is demonstrated using a model of an experimental high performance F/A-18 fighter aircraft with thrust vectoring. Redundant control surfaces have been reduced to two orthogonal control inputs (stability axis roll and yaw commands) by using the Pseudo Control method. Control synthesis is accomplished using Direct Eigenspace Assignment (DEA). The DEA control synthesis technique provides a mechanism to determine measurement feedback control gains that produce an achievable eigenspace for the closed-loop system.

In the CRAFT design process, the desired eigenspace is systematically varied over the complex plane, allowing the computation of metric values corresponding to each eigenspace specification. Metric values are numerical representations of design criteria. Metric surfaces are formed by plotting metric values corresponding to each frequency and damping point specified as a target eigenvalue. Graphical overlays of the metric surfaces are then used to show the best design compromise. Because the sensitivity of the metrics to pole placement is clearly displayed through surface gradients, the designer can readily assess the cost of tradeoffs among many metrics. This approach enhances the designer's ability to make informed design tradeoffs and to achieve effective final designs.

Introduction

Recent advances in aircraft technology are placing increasing demands on flight control design. Lighter structure for increased performance or less structure for low radar cross-section, the need for good flying qualities in extreme flight conditions, such as high angle-of-attack flight, demands for greater high-speed performance and for lower cost have all increased the complexity of the flight control design problem. Superimposed on these requirements, fighter aircraft have additional demands for agility, or enhanced maneuverability and controllability, resulting from advances in "point and shoot" weapons that are significantly changing air combat for the next generation of fighter aircraft. In the past, air combat engagements often resulted in tail-chase fights measured in minutes. Now engagements are measured in

seconds with combatants using all-aspect weapons. Future fighters may have to operate in environments where having substantial agility throughout a greatly expanded flight envelope is a requirement. Studies involving piloted and numerical air combat simulations (refs. 1–6) have shown that fighters with this capability are able to perform combat maneuvers in shorter time and in less space and thus achieve a tactical advantage. The demand for agility adds complexity to the control design problem. In addition, new control effectors, such as thrust vectoring and actuated nose strakes, offer the capability to achieve higher levels of agility than previously attainable, thus further complicating the control mix with redundant effectors that have varying effectiveness over the flight envelope.

Research efforts have focused on characterizing an aircraft's agility and defining high angle-of-attack flying qualities requirements. Many agility metrics have been proposed (refs. 7–14) for assessing combat capability, but they do not readily lend themselves for use in the control design process. Efforts to provide metrics for control law design have been reported in references 15–18 and have resulted in candidate design metrics and guidelines that have proven useful to a flight control law designer. In addition, several related studies have been performed as part of the NASA High Alpha Technology Program (HATP) (refs. 19–22). To achieve high levels of agility, including post-stall maneuvering capability, successful development and integration of several emerging technologies, such as thrust vectoring and highly integrated flight control systems, are required (ref. 23).

Successful completion of a control law design for systems incorporating these advanced capabilities requires control design methods that handle diverse design requirements. These design methods must allow the designer to conduct systematic tradeoffs to achieve a balanced design. This report describes a design methodology that uses a graphical approach to achieve a balanced design for systems where the design requirements can be quantified in the form of control design metrics. Control design metrics are quantitative measures of specific system capabilities that translate desired operational characteristics into useful engineering terms for control design. The design approach, referred to as CRAFT, stands for the design objectives addressed, namely, Control Power, Robustness, Agility, and Flying Qualities Tradeoffs. This approach, initially reported in reference 24, has been further developed and flight tested by application to the NASA High Alpha Research Vehicle (HARV). HARV is an experimental F/A-18 that uses both thrust vectoring and actuated nose strakes for enhanced high alpha control. This vehicle has a programmable flight computer on board that allows testing of different research control laws.

For the HARV flight experiments, feedback gains were designed for both the NASA-1A and the ANSER (Actuated Nose Strakes for Enhanced Rolling) control laws. For these flight experiments, a lateral-directional control law was developed using CRAFT in combination with Pseudo Controls (ref. 25). Pseudo Controls is a nonlinear control blending scheme that provides cooperative action among redundant controls while minimizing the number of feedback gains required and the complication of feedback gain schedules. Redundant control surfaces are reduced to two orthogonal control inputs by using the Pseudo Control method. Within the CRAFT feedback design process, the Pseudo Control system is linearized at design points to provide a linear matrix mapping between aircraft controls and the two orthogonal pseudo controls. A description of one control law, labeled NASA-1A, providing both architecture and simulation results, can be found in reference 26. This control law was used in the HARV thrust-vectoring-only experiments. A complete and detailed design specification for the ANSER control law, which included both thrust-vectoring and actuated nose strakes, is provided in reference 27.

The CRAFT methodology provides a coherent design process allowing the designer to judge the inevitable compromise among many different and often competing requirements. The process allows optimization of aircraft agility, manual control requirements, system tolerance to model error, and disturbance rejection, while at the same time respecting the limitations of finite control power.

Symbols and Abbreviations

a_j	denominator coefficients for observer-canonical form
A	plant matrix
A_n	plant matrix for nonphysical states
b_j	numerator coefficients for observer-canonical form
B	control distribution matrix for states
B_n	control distribution matrix for nonphysical states
C	state distribution matrix for outputs
$C_{L\alpha}$	nondimensional variation of lift coefficient with angle of attack
C_n	state distribution matrix for nonphysical outputs
D	control distribution matrix for outputs
E	uncertainty model
g	feedback gain
gm	gain metric based on sum of squares of gains
G	feedback gain matrix
G_x	maps states to controls, $G_x = [I_m - G\ N_c]^{-1}\ G\ M$
I	identity matrix (subscripts indicate dimension)
j	complex number $\left(j = \sqrt{-1}\right)$
K	plant compensation
KG	loop transfer matrix
L	matrix defining achievable subspace for ν
L'_p	roll moment due to roll rate, sec^{-1}
L'_β	roll moment due to sideslip angle, sec^{-2}
L'_δ	roll moment due to control input, sec^{-2}
m	number of controls
M	state distribution matrix for measurements
n	number of states
N	control distribution matrix for measurements

N'_r	yaw moment due to yaw rate, sec^{-1}
N'_β	yaw moment due to sideslip angle, sec^{-2}
N'_δ	yaw moment due to control input, sec^{-2}
p	number of outputs
p_{stab}	stability-axis roll rate, rad/sec
q	number of eigenvector elements specified
Q_{di}	weighting matrix to select elements of desired eigenvector
r	number of measurements
rad	radians
r_{stab}	stability-axis yaw rate, rad/sec
R^n	vector space of dimension n
s	Laplace variable, $s = j\omega$
T	scale matrix
$T_{\theta 2}$	flight path attitude lag parameter, sec
u	single control input
U	control vector ($m \times 1$)
v	side velocity, ft/sec
V	matrix of eigenvectors
V_o	trim velocity, ft/sec
w	desired eigenvector projection vector
W	matrix of w_i columns
X	state vector ($n \times 1$)
X_n	nonphysical state vector
Y	output vector ($p \times 1$)
Y'_β	side force due to sideslip angle, sec^{-1}
Y'_δ	side force due to control input, sec^{-1}
Z	measurement vector ($r \times 1$)
α	angle of attack, rad

β	sideslip, rad
δ	generic control input
Δ	transfer function denominator
ζ	damping ratio
θ	pitch angle, rad
λ	eigenvalue
λ_{roll}	roll mode eigenvalue
ν	eigenvector
$\underline{\sigma}$	minimum singular value
$\overline{\sigma}$	maximum singular value
ϕ_{stab}	stability axis bank angle, rad
ω	frequency, rad/sec
$\in$	element of set

Subscripts

a	achievable values
c	associated with controller
DR	Dutch roll
d	desired values
i	index over n modes
p	associated with pilot
s	scaled vector or matrix
ss	steady state

Superscripts

p	number of outputs
T	matrix transpose

Abbreviations

AOA	angle of attack, rad
CO	combat

CRAFT Control Power Robustness Agility and Flying Qualities Tradeoffs

DEA Direct Eigenspace Assignment

HARV High Alpha Research Vehicle

HATP High Alpha Technology Project

Mil-Std Military Standard Specifications

MIMO multiple input, multiple output system

rad radians

RMS root mean square

sec seconds

SISO single input, single output system

SSV structured singular value

Control Design Metrics

Mag agility metric for yawing motion

Mcp control power metric, defined as RMS magnitude of feedback gains

Mdr flying qualities metric for Dutch roll mode

Mri robustness metric for uncertainty at the inputs

Mro robustness metric for uncertainty at the outputs

CRAFT Design Method

CRAFT is a control law design approach that addresses key design objectives of concern to many flight control designers, namely, tradeoffs among control power, robustness, agility, and flying qualities requirements. This approach provides the designer with a graphical tool to simultaneously assess any quantifiable metric representing design objectives. The strength of this approach comes from the combined use of eigenspace assignment, which allows direct specification of eigenvalues and eigenvectors in the design, and graphical overlays of metric surfaces that capture the design goals in a composite illustration. Although eigenspace assignment facilitates this design process very efficiently, a number of design methods can be used to determine feedback gains in this approach. Designers must choose a control design algorithm and appropriate design metrics suited for each design problem.

In the CRAFT approach, design tradeoffs are made by interpreting graphical overlays of metric surfaces that quantitatively characterize each design goal. Numerous metrics from each of the key design objective areas can be applied simultaneously. Any unique metric reflecting a specialized requirement that can be expressed in engineering terms can be applied as well. Graphical overlays of the metric surfaces show the best design compromise for all the design criteria and clearly display the sensitivity of changing from that best-compromise design point. This feature can greatly enhance the designer's ability to make informed design tradeoffs.

Method Overview

CRAFT is summarized in block diagram form in figure 1. The design process begins by selecting a reasonable range of frequency and damping for the closed-loop dynamics of interest. For example, if a longitudinal design was desired, a range of frequency and damping for the short-period mode would be selected with the phugoid mode specified to meet Level 1 flying qualities. Within this range, a grid of design points is chosen to systematically cover the design space. Using eigenspace assignment as the control design algorithm, feedback gains are computed to achieve the desired dynamics for the closed-loop system at each design point. With eigenspace assignment, the designer must define both eigenvalues and eigenvectors; specifying the eigenvectors is discussed in sections "Eigenspace Selection" and "Design Issues." Once the desired closed-loop systems are determined for a specified set of frequency (ω) and damping ratio (ζ) pairs, each control design metric can be evaluated and plotted, producing a surface over the ζ-ω space. Some metrics, such as flying qualities specifications, may be known before the closed-loop design; however, the control power, robustness, and agility metrics require determination of the closed-loop system. Viewing the metric surface in a 2-D contour plot highlights the most desirable region to locate the short period pole with respect to the particular metric studied. The individual metric surfaces are an indication of the sensitivity of that metric to closed-loop pole location. A final overlay plot of desirable regions from each metric surface can then be obtained. This is represented by the bottom center block of figure 1. The intersection of desirable regions provides the best design compromise for all the design criteria considered.

One possible result of applying the CRAFT method is that some of the most desirable regions do not overlap. In such a case, a solution for all the metrics to be satisfied simultaneously does not exist, and therefore some compromise will be required. For example, the designer may feel it is better to give up Level 1 flying qualities to achieve acceptable robustness margins, or agility might be reduced to maintain acceptable flying qualities. With graphical overlays of metric surfaces, the designer is given a clear picture of both the sensitivities and impact of the tradeoffs being made. Although many metrics can be used, the designer can weight certain design metrics to achieve a desired final effect.

Control Synthesis Algorithm

In this study, the control synthesis algorithm is Direct Eigenspace Assignment (DEA), taken from reference 28. This control synthesis technique provides a mechanism to determine measurement feedback control gains that produce an achievable eigenspace for the closed-loop system. It has been shown (ref. 29) that, for a system that is observable and controllable with n states, m controls, and r measurements, one can exactly place r eigenvalues and m elements of their associated eigenvectors in the closed-loop system. DEA provides a mechanism to find achievable eigenvectors by placing q elements ($m < q < n$) of r eigenvectors associated with r eigenvalues through a least squares fit of the desired eigenvectors to the achievable eigenspace.

Consider the observable and controllable system expressed as

$$\dot{X} = A X + B_c U_c + B_p U_p \qquad (X \in R^n) \tag{1}$$

$$Y = C X + D_c U_c + D_p U_p \qquad (Y \in R^p) \tag{2}$$

with system measurements given by

$$Z = M\,X + N_c\,U_c + N_p\,U_p \qquad (Z \in R^r) \tag{3}$$

and a measurement feedback control law defined as

$$U_c = G\,Z \qquad (U_c \in R^m) \tag{4}$$

Substituting the measurement equation for Z into the expression for U_c, the controller input can then be written as a function of states, X, and pilot input, U_p,

$$U_c = G_x\,X + G_p\,U_p$$

where

$$G_x = [I_m - G\,N_c]^{-1}\,G\,M$$

$$G_p = [I_m - G\,N_c]^{-1}\,G\,N_p$$

Thus the closed-loop system becomes

$$\dot{X} = [A + B_c\,G_x]\,X + [B_p + B_c\,G_p]\,U_p \tag{5}$$

$$Y = [C + D_c\,G_x]\,X + [D_p + D_c\,G_p]\,U_p \tag{6}$$

$$Z = [M + N_c\,G_x]\,X + [N_p + N_c\,G_p]\,U_p \tag{7}$$

Spectral decomposition of the closed-loop system is given as

$$(A + B_c\,G_x)\,\nu_i = \lambda_i\,\nu_i \qquad (i = 1, 2, ..., n) \tag{8}$$

where λ_i is the ith system eigenvalue and ν_i is the associated ith system eigenvector.

This expression can be rearranged as

$$B_c\,G_x\,\nu_i = [I_n\,\lambda_i - A]\,\nu_i \qquad (i = 1, 2, ..., n) \tag{9}$$

and by defining w_i and L_i as

$$w_i = G_x\,\nu_i \tag{10a}$$

$$L_i = [I_n\,\lambda_i - A]^{-1}\,B_c \tag{10b}$$

the closed-loop eigenvector from equation (9) can be written in terms of w_i as

$$\nu_i = L_i\,w_i \tag{11}$$

The achievable eigenvector for the closed-loop system that reflects the desired eigenvalue and eigenvector specification (see fig. 2) can be written as

$$\nu_{ai} = L_{di}\, w_{ai} \tag{12}$$

where

$$L_{di} = [I_n\, \lambda_{di} - A]^{-1}\, B_c$$

By examining equation (12), one can see that the number of control variables (m) determines the dimension of the subspace in which the achievable eigenvectors must reside. Values of w_{ai} which yield an achievable eigenspace that is as close as possible to a desired eigenspace can be determined in a least squares sense. If ν_{di} is substituted for ν_{ai} in equation (12), the result is a weighted least squares problem for the unknown w_{ai}, for which the solution is

$$w_{ai} = [L_{di}^T\, Q_{di}\, L_{di}]^{-1}\, L_{di}^T\, Q_{di}\, \nu_{di} \tag{13}$$

where Q_{di} is a weighting matrix to select q elements of the eigenvector to be specified. With w_{ai} determined, the feedback gains producing the achievable dynamics can be obtained from equation (10a). After combining the column vectors for w_{ai} and ν_{ai} into matrices W and V, respectively, the gains are given by

$$G = W\, [M\, V + N_c\, W]^{-1} \tag{14}$$

The steps for determining feedback gains using DEA can be summarized as follows:

1) Select desired eigenvalues, λ_{di}, desired eigenvectors, ν_{di}, and desired eigenvector weighting matrices, Q_{di}.

2) Calculate w_{ai} using equation (13) and concatenate these columnwise to form W.

3) Calculate achievable eigenvectors, ν_{ai}, using equation (12) and concatenate these columnwise to form V.

4) Calculate the feedback gain matrix using equation (14).

Eigenspace Selection

Using eigenspace assignment requires proper selection of eigenvalues and eigenvectors. The eigenspace choice has a significant impact on feedback gains. As explained above, the target eigenvalue under study is specified over an appropriate ζ-ω space, while other system poles are held constant at desired values. The appropriate ζ-ω space and desired values for system poles are determined by engineering experience, understanding of the system dynamics, and familiarity with flying qualities data bases such as the Mil-Std 1797A (ref. 30). Flying qualities metrics specifying desirable values for aircraft rigid body modes are given for relatively low angles of attack (AOA) in Mil-Std 1797A. However, desirable values for modes in the high angle-of-attack regime ($\alpha > 20°$) are still a matter of research. Current research in this area can be found in references 17–18.

At the beginning of the design process some iteration may be required by the designer to determine the optimum values for the other system poles not designated as the target pole. However, experience has

shown that this issue is easy to resolve, especially if there is sufficient frequency separation between the target pole and other system poles. Nominal values for slow dynamics, such as phugoid or spiral modes, usually can be specified once with little effect on the best choice for the faster modes. A slow mode can be optimized quickly by designating it as the target pole for one iteration in the CRAFT process, if necessary.

Eigenvectors, on the other hand, need to be determined by the designer, and unfortunately, little guidance is available for determining the best eigenvectors. Although Mil-Std 1797A does not provide explicit guidance in the form of standard eigenvector specifications, it does provide a substantial body of design criteria which describes desirable classical dynamics for aircraft transfer functions. This data base, along with engineering experience, allows creation of design or "desired" eigenvectors. Mil-Std 1797A captures a long history of experience with aircraft and specifies desirable aircraft dynamics mostly in low order equivalent transfer function form. Transfer functions can be transformed to state-space form and thus can define the eigenspace. Unfortunately, until more experience is obtained with aircraft capable of high AOA, the Mil-Std for aircraft flying qualities is limited to providing low AOA design criteria. However, for defining eigenvectors, other options exist besides building up a "desired" state-space model from design criteria. The following sections introduce a few methods for specifying eigenvectors that have been used with the CRAFT method. These methods are categorized as (1) open-loop eigenvectors, (2) minimum-specification eigenvectors, and (3) desired-model eigenvectors. Results indicating some of the advantages and disadvantages for these different approaches are discussed in "Design Issues."

Open-Loop Eigenvectors

The first eigenvector selection method uses open-loop system eigenvectors. The open-loop eigenvectors may work in some cases where the open-loop system generally has desired classical aircraft responses but needs a small adjustment in pole placement. For example, eigenvalues and eigenvectors for the open-loop model at 5° AOA given in the appendix are provided in table 1. The model is a 4th order lateral-directional system representing the HARV, an experimental thrust-vectored F-18 fighter aircraft. States shown in table 1 are side slip, β (rad), stability axis roll rate, p_{stab} (rad/sec), stability axis yaw rate, r_{stab} (rad/sec), and stability axis bank angle, ϕ_{stab} (rad). Side velocity, used in the appendix, was converted to side slip angle in table 1 to make the discussion more tractable; however, all feedback gains in this study were computed using the models given in the appendix. Eigenvectors are expressed as magnitude and phase with the values normalized to the first element of the vector.

Table 1. HARV Open-Loop Eigenspace at 5° AOA

State	Dutch roll mode	Roll mode	Spiral mode
Open-Loop Eigenvalues			
not applicable	$-0.2070 \pm 1.6575j$	−1.4009	0.0043
Open-Loop Eigenvectors			
β	(1.0, 0.0)†	1.0	1.0
p_{stab}	(5.22, 133.99)	–67.74	1.62
r_{stab}	(1.57, –82.31)	3.86	20.18
ϕ_{stab}	(3.12, 36.87)	48.36	377.47

†(magnitude, phase [deg])

The open-loop model has a Dutch roll natural frequency of 1.67 rad/sec and a damping ratio of 0.12. For closed- loop dynamics, much more damping is required to meet Level 1 flying qualities requirements

for fighter aircraft in combat maneuvering (Class IV aircraft, CO phase). The Dutch roll damping ratio must be greater than 0.4 and the natural frequency must be greater than 1.0 rad/sec. This represents a case where a viable design could be made using open-loop eigenvectors and simply compensating for a lack of Dutch roll damping. The eigenvectors show a fairly classical and desirable character, because the roll mode is dominated by roll rate with very little side slip, and the Dutch roll mode has a desirable ϕ/β ratio of about 3.0 (ref. 30). Thus, a designer could use these eigenvectors in a design specification with the appropriate eigenvalues specified. An advantage of this approach is a straight-forward design process and possibly very low feedback gains if the poles are not specified too far from the open-loop values.

Minimum-Specification Eigenvectors

The second eigenvector selection method is a straight forward technique that uses eigenvectors defined by zeroes and ones. Each element of the eigenvector is chosen to be 0 or 1, as appropriate, to achieve desired decoupling of the aircraft rigid body modes and to maintain linear independence of the eigenvectors. For a design using the lateral-directional model in the appendix, the choice would reflect the desire to decouple roll and Dutch roll modes. Specifying 0's or 1's in the "desired" eigenvector can be done with eigenspace assignment, since the method will provide the closest achievable eigenvector to that "desired" eigenvector. Minimum-specification eigenvectors have been used with success by Shapiro and others in application to flight control design (refs. 31, 32). In references 26 and 27, this design approach was used effectively for lateral-directional design of eigenvectors, but with modification, to provide appropriate ϕ/β ratio over the CRAFT design space and to minimize gain magnitudes.

In reference 26, initial elements for eigenvectors were chosen as shown in table 2, where the states for this table are the same as for the previous case using open-loop eigenvectors. An element free to be determined by the eigenspace assignment algorithm was indicated by "x.x," while the other elements were as specified in table 2. The choice of 0's and 1's follows from a desire to have no sideslip present in the roll mode and spiral mode responses and to have a specified ϕ/β ratio in the Dutch roll response.

Table 2. HARV Desired Closed-Loop Eigenspace at 5° AOA

State	Dutch roll mode	Roll mode	Spiral mode
Desired Closed-Loop Eigenvalues			
not applicable	$-1.170 \pm 1.194j$	−2.2	−0.004
Minimum-Specification Eigenvectors*			
β	(1.0, 0.0)†	0.0	0.0
p_{stab}	(x.x, x.x)	1.0	x.x
r_{stab}	(x.x, x.x)	x.x	x.x
ϕ_{stab}	(3.0, 0.0)	x.x	1.0

*x.x represents unspecified elements, †(magnitude, phase [deg])

The desired closed-loop eigenvalues reflect the requirements for Level 1 dynamics according to Mil-Std 1797A. As shown in table 2, the roll mode has been made substantially faster at 2.2 rad/sec, and the Dutch roll mode has an improved damping ratio from 0.12 to 0.7, while maintaining the same natural frequency, 1.67 rad/sec, as in the open-loop case.

Desired-Model Eigenvectors

The third eigenvector selection method considered is referred to as the desired-model method. This method has many variations that have been used with some success. The geneses of all the desired-model methods start with specification of desired transfer functions for the system. Three variations of the desired-model methods are discussed in this section: (1) explicit 4th order state-space expression, (2) transfer function replacement, and (3) observer-canonical form. For each variation, after a transfer function build-up of the desired input-output relationships, a transformation to a state-space system must be performed. The system matrix obtained from this transformation is then used to determine the eigenvectors. This process can be accomplished in a variety of ways, but for brevity, only three approaches for desired-model eigenvectors are suggested, using a lateral-directional model.

In the first desired-model approach, the transformation is accomplished by explicitly defining expressions for the system matrix in terms of desired eigenvalues. This is substantially different from the remaining two approaches in that the transformation is specified analytically. In the second and third approaches, the designer defines transfer functions in terms of gains, poles, and zeroes for all the input-output pairs and then transforms to state-space form. Because this transformation is not unique, an issue confronts the designer regarding how to obtain the aircraft physical states after transforming to state-space form. A means to resolve this issue is provided with these two approaches, transfer function replacement and observer-canonical form.

Explicit 4th order state-space expression. The first desired-model approach provides an expression for the system matrix in terms of the desired transfer function dynamics and thereby incorporates the transformation between state-space and transfer function form explicitly. The result is an expression of the system matrix in terms of desired frequency and damping, from which eigenvectors can be determined.

With simplifying assumptions of no gravity and zero pitch angle, a 3rd order lateral-directional model can be written as

$$\begin{bmatrix} \dot{\beta} \\ \dot{p} \\ \dot{r} \end{bmatrix} = \begin{bmatrix} Y'_{\beta} & 0 & -1 \\ L'_{\beta} & L'_{p} & 0 \\ N'_{\beta} & 0 & N'_{r} \end{bmatrix} \begin{bmatrix} \beta \\ p \\ r \end{bmatrix} + \begin{bmatrix} Y'_{\delta} \\ L'_{\delta} \\ N'_{\delta} \end{bmatrix} \tag{15}$$

This form of the model allows expressions to be derived for transfer functions after applying Laplace transformation to equation (15). In this derivation, δ represents a lateral-directional control input, and prime notation indicates that dimensional derivatives have been divided by appropriate mass or inertial terms consistent with units of equation (15). The resulting characteristic equation, Δ, for all the input-output pairs is found to be

$$\Delta = \left(s - L'_{p}\right)\left[s^2 - s\left(Y'_{\beta} + N'_{r}\right) + \left(N'_{\beta} + Y'_{\beta}N'_{r}\right)\right] \tag{16}$$

where the classical airplane poles for the Dutch roll and roll subsidence modes can be identified. In this case, frequency and damping for roll and Dutch roll modes can be equated to the terms in equation (16) as

$$\text{roll mode:} \qquad L'_{p} = \lambda_{roll}$$

Dutch roll mode: $Y'_\beta = N'_r = -\zeta\omega$

$$N'_\beta = \omega^2(1-\zeta^2)$$

where the assumption is made that Y'_β and N'_r are of equal magnitude. This assumption allows straight-forward solution for ζ and ω; however, the degree of validity may vary with each problem. The result is that the closed-loop system matrix A, shown in equation (17), produces the desired eigenspace. In order to obtain a 4th order system, the spiral mode can be appended by adding bank angle as the 4th state. This leads to a final 4th order system matrix that has the desired eigenvalues and can be used to determine the corresponding desired eigenvectors. This final system matrix can be written as

$$A = \begin{bmatrix} -\zeta\omega & 0 & -1 & 0 \\ L'_\beta & \lambda_{roll} & 0 & 0 \\ \omega^2(1-\zeta^2) & 0 & -\zeta\omega & 0 \\ 0 & 1 & 0 & \lambda_{spiral} \end{bmatrix} \tag{17}$$

The simplifying assumptions used to obtain A are appropriate for a broad range of AOA, considering the intended use of A. Although the system matrix, A, is derived assuming low AOA, it is representative of a classical and desirable set of aircraft dynamics that are likely to be desirable over a wide range of AOA. However, it is currently a matter of research to determine what modal characteristics are desirable for high AOA. The system matrix is only used as a target system for design. The target system has desirable modal characteristics that the eigenspace assignment algorithm matches within the constraints of the aircraft system capabilities. As long as desirable modal characteristics are expressed in the target system, successful designs can be achieved.

Transfer function replacement. The second desired-model approach requires more computation and engineering judgment than the first. Building transfer functions may be accomplished efficiently by transforming the open-loop state-space system to transfer function form and then correcting any undesirable values of gains, poles, or zeroes. In transfer function form, the designer must specify the desired gains, poles, and zeroes for each input-output relationship using information from the Mil-Std 1797A or from system knowledge and experience. Because this approach will allow any desired specification to be made, the zeroes need to be specified within limits that make physical sense for the aircraft, otherwise unreasonably high feedback gains may result. After appropriate specifications are made, a transformation back to state space can be performed. This step causes a loss of information because the transformation back to state space is not unique. In other words, the states after transformation are not [β p r ϕ]. The inputs and outputs of the system are the same, however. Define a desired single-input, multi-output, state-space system with physical states ([β p r ϕ]) as

$$\dot{X} = A\,X + Bu \tag{18}$$

$$Y = C\,X \tag{19}$$

and define the nonphysical state-space model obtained from transforming the desired transfer functions back to state space as

$$\dot{X}_n = A_n\,X_n + B_n\,u \tag{20}$$

$$Y = C_n\,X_n \tag{21}$$

It is possible to map back to the original state-space model if C_n can be inverted and the outputs, Y, are the desired physical states, X. Thus,

$$X_n = C_n^{-1} Y = C_n^{-1} X \tag{22}$$

Substituting this expression into the nonphysical state equation (20) produces the desired similarity transform

$$\dot{X} = C_n A_n C_n^{-1} X + C_n B_n u \tag{23}$$

which is the desired state equation.

One issue that arises in this process of transforming back to state-space is the production of different C_n coefficients in equation (21) corresponding to each input, u. This leads to the question of which C_n to use in equation (22) for systems with multiple inputs. Fortunately, the A_n is identical for each input-output pair because the A_n matrix represents a direct mapping from the system poles. The poles form a common denominator for all the system transfer functions, i.e., for each input-output pair. The B_n matrix is different for each transfer function, but B_n simply becomes a new column in the final desired B matrix after the matrix multiplication $C_n B_n$. The C_n matrix, however, presents a problem because it is desirable to have only one matrix mapping from states to outputs. One method to address this issue is to use C_n associated with lateral stick input in the similarity transform of equation (23) to determine the system matrix that will define effective eigenvectors for the roll and spiral modes. Similarly, use C_n associated with rudder pedal inputs for the definition of Dutch roll eigenvectors.

Observer-canonical form. The third desired-model approach offers another way to resolve the nonunique transformation from transfer function to state-space. This is done by using the observer-canonical form to map transfer functions to state-space equations. This form defines the state-space system in terms of the transfer function polynomial coefficients for the numerator and denominator. For a single-input, single-output (SISO) model, the observer-canonical form is

$$A_1 = \begin{bmatrix} \cdots 0 \cdots & -a_0 \\ \ddots & \vdots \\ I & -a_{n-2} \\ & \ddots\, -a_{n-1} \end{bmatrix}, B_1 = \begin{bmatrix} b_0 - b_n a_0 \\ \vdots \\ b_{n-2} - b_n a_{n-2} \\ b_{n-1} - b_n a_{n-1} \end{bmatrix}, C_1 = \begin{bmatrix} 0 & 0 & \cdots & 1 \end{bmatrix},\ D_1 = \begin{bmatrix} b_n \end{bmatrix} \tag{24a}$$

where a_i are the denominator coefficients and b_j are numerator coefficients. For aircraft state equations b_n will be zero. For the multi-input case, each new input is represented by a new column in B and D corresponding to b_j numerator coefficients. For the multi-output case, each new output creates an additional row in C as well as an additional block in A, B, and D, as shown in equation (24b).

$$A = \begin{bmatrix} A_1 & \\ \hdashline & A_2 \end{bmatrix},\ B = \begin{bmatrix} B_1 \\ \hdashline B_2 \end{bmatrix},\ C = \begin{bmatrix} C_1 \\ \hdashline C_2 \end{bmatrix},\ D = \begin{bmatrix} D_1 \\ \hdashline D_2 \end{bmatrix} \tag{24b}$$

Reference 33 covers this canonical form for multi-input, multi-output (MIMO) systems. With this type of mapping, the complete set of desired transfer functions can be directly mapped into state-space form; however, the order of the model is greatly increased. Using standard model reduction techniques to obtain a minimal realization, a complete 4th order state-space model can be obtained with approximately

the desired dynamics. By choosing the system outputs to be the aircraft states of interest, this system can then be transformed back to aircraft physical states using the similarity transform shown for the transfer function replacement approach, equation (23).

Control Design Metrics

Control design metrics quantify control design goals and are an integral part of the CRAFT Design Method. Many control design metrics exist for aircraft and most fit into one of four design objective areas characterizing control power, robustness, agility, or flying qualities. In this paper a representative metric is proposed for each design objective area and demonstrated in examples. Clearly, many more metrics exist and may be required for a particular design problem. For tractability, the design example in this paper is limited in the number of metrics applied.

Control Power Metrics

Control power metrics characterize the forces and moments required to achieve certain dynamics with a given aircraft. The metric chosen for this study is based on a Frobenius norm of gains that indirectly represents a measure of control power required to achieve the desired eigenspace. The assumption is made that larger gains generally correspond to a demand for greater control deflection or deflection rate, and this, in turn, reflects a demand for greater control power. For this metric, smaller values are more desirable, since small gains reflect reduced control power demands. The expression for the gain metric is given as

$$gm(\zeta,\omega,\nu) = \frac{1}{\sqrt{m * n}} \sqrt{\sum_{i=j}^{m} \sum_{j=1}^{n} g_{ij}^2(\zeta,\omega,\nu)} \tag{25}$$

where $g_{ij}(\zeta,\omega,\nu)$ is an element of the $m \times n$ feedback gain matrix determined using eigenspace assignment. The feedback gains are a function of the particular eigenvalues and eigenvectors (represented as ζ, ω, and ν) chosen for each CRAFT design point. If desired, a weighting matrix to selectively emphasize or eliminate certain gains from the analysis could be included. In this case, the leading factor in equation (25) scales the Frobenius norm to provide an RMS gain value.

Robustness Metrics

An important concern to control designers is that the control system tolerate the inevitable model error associated with mathematical descriptions of physical systems, as well as reject disturbances and measurement noise. Model error has several sources, but certainly one source of concern is the limited fidelity of low-order, linear, time-invariant models in representing the actual aircraft, especially at off-design points in the flight envelope. These models, typically used in design, cannot fully capture the strong nonlinearities that exist in aerodynamic models at high angles of attack. Consequently, the designer must respect these limitations or aggravate the robustness problem. Fighter aircraft experience additional nonlinear characteristics, such as inertial coupling due to very high roll rates and relatively high angles of attack. Multivariable stability robustness is an especially important design consideration for high angle-of-attack and high agility aircraft.

A variety of metrics can be used to indicate the regions in the ζ-ω design space with the greatest tolerance to model error. Unstructured uncertainties, in the form of multiplicative error models at the input and output, may be satisfactory for initial designs. For a given error model, singular values of the

inverse return difference matrix provide an easily computed, general robustness metric. Structured uncertainties would provide less conservative measures for configuration-specific cases; however, more computation and user knowledge of the uncertainties are needed in that case. An example application of structured singular values (SSV) as a robustness metric is given in reference 26, where SSV are used as a CRAFT design metric for the HARV control laws. Although more conservatism than generally desired is obtained with unstructured uncertainty models, some benefit is obtained by erring on the conservative side for initial designs. The more conservative metric yields a smaller desirable region in the ζ-ω space. Therefore the designer has some confidence that being on or near the edge of that conservative region is not prohibitive.

A candidate robustness metric for this report, using unstructured singular values, is determined from the minimum singular value given as $\underline{\sigma}[I + [K(s)G(s)]^{-1}]$, where K(s)G(s) is the loop transfer matrix. In using these metrics a designer would consider the peaks as regions with the most promise for robustness over the ζ-ω space considered. If an uncertainty model, E(s), were available, it could be applied to determine the regions of guaranteed stability. A sufficient condition for stability is $\underline{\sigma}[I + [K(s)G(s)]^{-1}] > \bar{\sigma}\ [E(s)]$ for $s = j\omega$. Because an uncertainty model is not always available, this metric is chosen to highlight the regions with the most promise, that is, the regions where the metric has greatest value. It is possible, however, to show that metric values of 0.5 correspond to a multivariable equivalent of 6 dB gain margin and 30° phase margin (ref. 34). Therefore, it is reasonable to view regions of the robustness metric with values greater than 0.5 to be desirable regions.

Agility Metrics

For this study, the design objective area for agility is restricted to airframe agility. These agility metrics, unlike many in the literature, do not reflect pilot compensation effects. This was done intentionally to allow separation of flying qualities and agility metrics. This approach enhances a "building block" design philosophy where the designer can choose to add or delete varying degrees of any characteristic by selecting the appropriate metrics. Thus, design freedom exists within regions of Level 1 flying qualities (or Level 2 if Level 1 cannot be achieved) to select the desired level of airframe agility. The agility metrics in combination with the flying qualities metrics aid the designer in selecting the most agile aircraft within the limitations of a pilot.

Some controversy exists on the exact definition of agility and which parameters best describe it (ref. 35). This reflects the limited experience of both the operational and research communities with advanced agile fighters capable of high angles of attack. A significant experience base is needed, involving air combat aircraft capable of high-α flight, using, for example, thrust vectoring and all aspect weapons, before precise definitions become established. Even without the precise definition, many agree that angular accelerations characterize an important aspect of transient agility. For this reason, an acceleration metric is suggested as one of the agility metrics that should be considered in a CRAFT design. Many other metrics, such as maximum rates or displacements, may be appropriate in a particular design and can easily be accommodated in CRAFT.

The agility metrics described in this paper represent an average rotational acceleration characterizing roll or yaw accelerations in the lateral-directional axis. These metrics represent a blend of transient and functional agility characteristics and are just one type among many in the literature. Agility metrics for each of the three axes can be computed similarly with only minor differences that reflect the different nature of longitudinal, lateral, and directional axes.

The yaw acceleration metric is computed as peak stability-axis yaw rate divided by the corresponding time to peak. The pitch acceleration metric (not used in this paper) can be computed in the same fashion. The roll acceleration metric is computed by taking an average of the stability-axis roll acceleration over a specified period of time. Computing an average roll acceleration avoids determining a time-to-peak for roll rate. This is advantageous because roll response is typically designed to behave as a 1st order response. In any case, each metric has its values determined using the response to a step input at each design point in the CRAFT design space.

Some additional modification to agility metric computation is required, however, to ensure a valid comparison of metric values. If used directly, the agility metrics described above may lead the designer to choose low damping ratios or low frequencies for the target pole in order to obtain greater accelerations. This can be seen by considering the system equations (26) and controller equation (27) given as

$$\dot{X} = A X + B_c U_c + B_p G_p U_p \tag{26a}$$

$$Y = C X \tag{26b}$$

$$U_c = GY \tag{27}$$

The resulting closed-loop system produces a steady-state response to a step pilot input U_p, given as

$$Y_{ss} = -C[A + B_c G C]^{-1} B_p G_p U_p \tag{28}$$

which implies reduced response levels as feedback gain magnitude, G, is increased. Because feedback gains have been designed in the feedback path, the increased gain required to achieve pole placement at higher frequencies also produces reduced response magnitudes. In this case, high gains required for faster poles and therefore greater accelerations result in lower peak rates. The result, in terms of the metrics, is that larger values of peak rate occur at lower frequency and dominate the metric plot.

To make the metric comparisons valid, steady-state displacement of the response variable is forced to the same displacement at each design point. For example, in the longitudinal axis a steady-state pitch angle is specified, and for the directional axis a steady-state sideslip angle (β_{ss}) is defined. In this study, β_{ss} is specified to be 10°. In the lateral axis, a steady-state roll rate is used with a value of 1 rad/sec. Forcing the same steady-state displacement (or rate for the lateral axis) requires, in effect, a "gearing change" to be reflected in the closed-loop control distribution matrix. This is accomplished by multiplying B_p by the G_p gain. This allows the designer to adjust Y_{ss} to desired values.

Flying Qualities Metrics

The fourth design objective area addresses pilot-in-the-loop issues that are usually quantified by flying qualities metrics. Flying qualities metrics help the designer assess the best tradeoff between pilot workload and system performance. Although a large data base exists for flying qualities metrics at low angles of attack, such as Mil-Std 1797A (ref. 30), the data base is virtually nonexistent beyond relatively modest (>20°) angles of attack. Research to develop flying qualities criteria at high angles of attack, supported by NASA, has been reported in references 16–18.

Figures 3(a) and 3(b) show flying qualities specifications that define desirable regions for the roll mode time constant and Dutch roll mode, respectively. These metrics are taken from Moorhouse-Moran (ref. 36), Mil-Std 1797A (ref. 30), and McDonnell Aircraft (refs. 37, 38). The Mil-Std Level 1 and Level 2 regions represent the largest areas in figure 3(a). The desirable regions used in the Moorhouse-Moran study are much smaller than the Mil-Std because of the restricted nature of the tasks considered; these tasks were specifically tailored to modern high-performance fighter missions. Both the Moorhouse-Moran and the Mil-Std values are for the low angle-of-attack case. The smallest region in figure 3(a), shown as an elliptic area, reflects the even more restricted nature of the tasks used by McDonnell Aircraft to specifically define lateral gross acquisition dynamics for a modern high performance fighter at low angle of attack. Initial studies by McDonnell Aircraft investigating desirable roll mode time constants for fighter aircraft at 30° angle of attack are shown as solid lines defining Level 1 and Level 2 boundaries for the region considered (refs. 37, 38). These results have been updated and extended to other angles of attack in reference 18. Figure 3(b) provides Dutch roll mode specifications from both Mil-Std 1797A and Moorhouse-Moran. Again the more restrictive nature of the tasks used in the Moorhouse-Moran study lead to a smaller area for Level 1 flying qualities.

Design Example

The design example presented in this paper highlights the facility that CRAFT provides to the designer in achieving the desired closed-loop dynamic characteristics. The technique is applied to a lateral-directional model using the explicit form of the desired-model eigenvector approach for eigenspace selection. The ramifications of choosing this approach over the other approaches discussed previously are considered in the “Design Issues” section.

To demonstrate the CRAFT method, a single-point design applying CRAFT to a 4th order linear model of HARV, trimmed at 30° angle of attack, is presented. The open-loop plant is defined in the appendix. The system states are side velocity (ft/sec), stability axis roll rate (rad/sec), stability axis yaw rate (rad/sec) and stability axis bank angle (rad). Inputs are vlat and vdir, the Pseudo Controls representing lateral and directional commands. These control inputs are normalized acceleration commands and represent the pilot’s commands to lateral stick and pedal after crossfeeds, shaping, feedbacks, and appropriate filtering are done. Feedback measurements are stability axis roll rate (rad/sec), stability axis yaw rate (rad/sec), lateral acceleration (g’s), and sideslip rate (rad/sec). Full state feedback is not required because CRAFT has been configured with DEA that only requires independent measurements and controls.

Design Specifications

Design specifications enter into the CRAFT design method as control design metrics. For this example, only one metric from each of the four design objective areas is considered. In a more complete design, many metrics from each design objective area would be considered. The design metrics for each of the four design areas are representative metrics used in design applications. The flying qualities metrics described in figure 3 define a recommended range of pole locations for the CRAFT design. For this example, the desired Dutch roll mode damping ratio is varied from 0.1 to 0.9 and the natural frequency is varied from 0.4 rad/sec to 2.4 rad/sec, which gives reasonable coverage to the range of possible pole locations appropriate for the system under study. Dutch roll frequency is limited to 2.4 rad/sec because analysis shows the feedback gains become unacceptable for larger values. The roll mode is varied from –0.2 to –4.2 rad/sec, which corresponds to a roll mode time constant range of 5.0 sec to 0.238 sec. The range of values (0.2 to 1.6 sec) shown in figure 3(a) gives complete coverage to the

recommended range based on results from the McDonnell Aircraft simulation study at 30° angle of attack (ref. 38).

Eigenvalues and eigenvectors for the open-loop, 30° AOA model are provided in table 3. States shown in table 3 are sideslip, β (rad), stability axis roll rate, p_{stab} (rad/sec), stability axis yaw rate, r_{stab} (rad/sec), and stability axis bank angle, ϕ_{stab} (rad). To make this discussion of eigenvectors more tractable, side velocity was converted to sideslip angle for presentation in table 3. However, all CRAFT calculations for this paper were done using the models as given in the appendix. Eigenvectors are expressed as magnitude and phase with the values normalized to the first element (β) of the vector.

Table 3. HARV Open-Loop Eigenspace at 30° AOA

State	Dutch roll mode	Roll mode	Spiral mode
Open-Loop Eigenvalues (α = 30°)			
not applicable	$-0.3465 \pm 1.2058j$	−0.2045	−0.0549
Open-Loop Eigenvectors (α = 30°)			
β	(1.0, 0.0)†	1.0	1.0
p_{stab}	(2.13, 112.96)	−4.26	−1.35
r_{stab}	(1.28, 292.98)	2.58	2.99
ϕ_{stab}	(1.72, 6.93)	21.17	26.14

†(magnitude, phase [deg])

This model has a satisfactory spiral mode pole at -0.0549 sec^{-1} for a time-to-half of 12.6 sec. A Level 1 value for this mode (ref. 30) requires a minimum time-to-double amplitude of 12 sec and a suggested limit on time-to-half amplitude of 10 sec. For convenience in the analysis of this problem, the spiral mode pole is specified to be -0.05 sec^{-1}. This value more than satisfies Level 1 requirements and does not significantly modify the feedback gain calculations. The roll mode pole is initially set at -1.4 sec^{-1} (roll mode time constant of 0.71 sec) based on achievable roll rates and high-alpha roll mode time constant recommendations from figure 3(a) (ref. 38). This can be optimized by CRAFT after the desired Dutch roll mode characteristics have been determined. A second iteration using the "best" Dutch roll mode and allowing the CRAFT process to sweep over possible roll mode values determines the "best" value for the roll mode.

Eigenvectors are chosen using the explicit eigenvector specification approach, although for ease of design it may often be more desirable to use the minimum-specification approach with ϕ/β optimization. Optimization of ϕ/β ensures lower overall gain magnitudes and improved ϕ/β ratios. This procedure for defining eigenvectors and other optional procedures are discussed in the "Design Issues" section of this report. Regardless of the method chosen, eigenspace specifications are consistently determined over the ζ-ω space for each new target pole location; then with the eigenspace specified, the feedback gains to achieve each Dutch roll pole location are determined over the ζ-ω space of interest.

Once closed-loop systems are determined, metrics can be evaluated at each point over the ζ-ω space and a corresponding surface plotted to determine the metric sensitivity to pole location as well as the desirable regions to place the target pole, in this case the Dutch roll pole. Figure 4 presents four metric surfaces corresponding to each design objective area except for the flying qualities area, which was shown in figure 3. Each graph shows a 3-D mesh plot of the metric surfaces to enable easy visualization of the surface. Corresponding 2-D contour plots are shown in figure 5 to highlight the most desirable regions. Metric magnitudes are indicated on the contour lines to highlight variation of the metric over the complex plane.

Control Power—Dutch Roll Mode

The upper left-hand graphics of figures 4 and 5 present the control power metric from the first design objective area; these graphs are labeled as "Mcp" as a function of frequency and damping ratio. For this design example, Mcp was defined as a gain metric given by equation (25) and all feedback gains were equally weighted in the calculations. Plotted in this fashion the metric is a sensitivity measure indicating desirable regions for the Dutch roll pole and preferred directions to move the pole if an adjustment is desired. This surface gives an indication of where, in terms of pole placement, the greatest control power demands will be placed on the control system. Low values of Mcp correspond to desirable values (reduced gains), and high values in the high frequency region correspond to undesirable values (high gains) and greater required control power. The lower damping ratios are favored in the sense of reducing gain magnitudes; these values are closer to the open-loop value of the system.

For this eigenspace configuration and the target region considered, wide latitude exists for the choice of damping with respect to control power. Relatively small gain metric values (Mcp < 2.0) fall in the frequency range of 0.6 to 1.6 rad/sec for all damping ratios considered. High frequency requirements will drive up control power required. The most desirable region naturally tends to be an area near the open-loop pole where no feedback is required. If the open-loop eigenvectors had been chosen, zero gains would be required for the point at $(\zeta, \omega) = (0.28, 1.25)$. For this example, however, the gain metric does not go exactly to zero at the open-loop pole location because some feedback is still required to achieve the desired eigenvector specification that does not correspond to the open-loop case.

Robustness—Dutch Roll Mode

For this example, robustness metrics for uncertainty at the inputs and outputs were determined based on unstructured uncertainty models discussed in the "Robustness Metrics" section of this report. These robustness measures are shown over a range of frequency and damping for the Dutch roll mode on the bottom left- and right- hand sides of figures 4 and 5. The robustness metric is labeled "Mri" for uncertainty at the input and "Mro" for uncertainty at the output.

Figure 5(c) shows that Mri, robustness to uncertainty at the inputs, begins to deteriorate with Dutch roll frequencies above 1.6 rad/sec, but is well above the suggested datum of 0.5 for all values of frequency and damping considered. For this example, Mri does not provide a hard design constraint; consequently, the designer has flexibility in choosing the Dutch roll mode with respect to this metric. On the other hand, Mro, the robustness to uncertainty at the outputs, meets the 0.5 datum only in a region between 1.2 and 1.45 rad/sec. Considering both robustness design metrics together, a fairly large desirable region for Dutch roll frequency is obtained between 1.2 and 1.45 rad/sec.

Agility—Dutch Roll Mode

The graphic in the upper right hand corner of figure 4 presents the airframe yaw agility metric, Mag. Roll agility is not presented because there is little sensitivity of roll agility to Dutch roll mode placement given the eigenspace chosen for this example. For the yaw agility metric, progressively greater values show the more desirable values of agility, i.e., greater yaw acceleration. The 2-D contour plot, figure 5(b), has contour lines quantifying the value of the metric. As expected, the contour lines indicate that increasing frequency and reducing damping will improve yaw agility. For maximum agility the most desirable region is located at the lower right-hand portion of the figure, where Mag ranges from 0.4 rad/sec^2 to 0.5 rad/sec^2. Care must be used when comparing these metric values with measured or simulated instantaneous values of yaw acceleration. This Mag is an average acceleration produced from a

step input. In addition, the input is adjusted to provide the same steady-state sideslip angle for each pole location. Consequently, incorrect conclusions could result from a direct comparison with instantaneous simulated or measured values. Design experience will indicate the best values for this metric; however, sensitivity information is contained in the plot, and it provides an indicator of the best direction to move the poles for increasing agility. In this example, the agility metric indicates that, to achieve the most yaw agility, the designer should choose the highest frequency and lowest damping that still satisfies the other metrics.

Flying Qualities—Dutch Roll Mode

The fourth design objective area covers pilot-in-the-loop requirements. A presentation of flying qualities specifications for the roll and Dutch roll modes is given in figure 3. Included in this figure are roll mode specifications for gross acquisition at 30° AOA. Because no high AOA design guidelines exist for the Dutch roll mode, the requirement for low feedback gain magnitudes (i.e., Mcp) will be weighted heavily. In addition, the low AOA flying qualities requirements for Dutch roll frequency and damping will be satisfied only if no contradiction exists with the other metrics. Given this design viewpoint, the Moorhouse-Moran suggested minimum Dutch roll frequency of 1.0 rad/sec will be readily satisfied.

For this example, the flying qualities metrics are known before the design closed-loop systems are calculated. Although no flying qualities metrics need to be calculated for the closed-loop system, a designer may choose to apply other criteria that may require computation. For example, criteria such as Neal-Smith, Smith-Geddes, or Backdrop criteria (refs. 39–41) could be applied in a longitudinal problem.

Composite/Contour Overlay—Final Design—Dutch Roll Mode

For this example problem, only five metrics are involved, and an astute designer may quickly determine the best design compromise by just considering figures 3–5. However, in a general design problem many more metrics may be involved, making the analysis more difficult. In the CRAFT design approach, to make determination of the best design region for a target pole more tractable, a composite metric surface is formed over the ζ-ω design space.

The CRAFT composite surface reflects all the metrics by increasing in value where desirable-metric regions overlap and where the net sum of metrics is increasing. The composite surface is formed by first normalizing all metric surfaces shown in figure 4 to unity, i.e., the best (usually the largest) value is set to one. Dutch roll flying qualities specification (labeled “Mdr” in figure 6), is represented as a flat surface equal to one and is used to reflect the Level 1 region ($\zeta_{DR} > 0.4$, $\omega_{DR} > 1.0$) of the flying qualities metric defined in figure 3(b). The normalized metric surfaces are then summed together. If a metric has the convention of increasing positive values indicating improvement, it can be summed directly. If a metric such as the control power metric, Mcp, is included, it must be modified to the same convention before being added to the composite surface. Because Mcp has an improving value as the metric value becomes smaller, it requires an “inversion” before being added to the composite. This is accomplished by subtracting the normalized metric from one. The result is that the new metric now has larger values close to one as the control power required becomes more favorable, i.e., as control power required is reduced.

For this example problem, figure 6(a) shows the composite metric surface. Since all 5 metrics are represented in this figure, a maximum value close to 5 is possible but not likely, because that would require the best points of each metric to occur at the same values of ζ and ω. One variation on this process is to have weights multiply the normalized metrics to reflect individual designer requirements. No weights are used in this example.

The "best" design choice is a region where all metric desirable regions overlap with their greatest values. In practice, it is not likely to have all the desirable regions overlap, so the best design choice is where most metric desirable regions overlap. The best region is easily seen by considering a contour representation of the composite surface, as shown in figure 6(b), "Composite metric contours." In this graphic the best design region is centered on $\omega = 1.3$ and extends from $\zeta = 0.4$ to 0.8, with the peak occurring at $(\zeta, \omega) = (0.4, 1.3)$. A smaller or more definitive best design region could be determined by using contours with more resolution; however, little is gained in the final analysis. Using designer's discretion, composite metric values greater than 3.0 will be considered adequate and greater than 3.5 as most desirable.

The designer's final decision can be simplified by observing some of the key desirable regions superimposed over the composite metric contour graphic. The most desirable regions of all five metrics in figures 3 and 5 are shown together in figure 6(c), "Metric desired regions." For this design example, the desirable region for the control power metric, Mcp, was chosen to be $Mcp \leq 1.0$. This region corresponds to the contour labeled as "1" in both figures 5(a) and 6(c). The desirable region for both robustness metrics was chosen as the region with magnitudes ≥ 0.5. For Mro, this region is defined by two vertical solid-line contours labeled as "0.5" in figures 5(d), 6(c), and 6(d). The other robustness metric, Mri, was satisfactory over the entire region considered and therefore its contour is not shown in figure 6. In this graphic, the most desirable regions of all the metrics overlap except for the agility metric, Mag, which has its largest values (0.4–0.5 rad/sec^2) in the low damping and high frequency region. Unfortunately, very limited specifications exist for agility of advanced fighter aircraft, and no specification exists for this specific metric. However, experience with HARV indicates that values of 0.1 to 0.2 rad/sec^2 may be acceptable for this metric when considering HARV-like aircraft at 30°AOA. The fifth metric used in this example is the flying qualities metric, shown as dashed lines in figure 6(c) and labeled as Mdr, defining Level 1 to be where $\zeta_{DR} > 0.4$ and $\omega_{DR} > 1.0$ for the Dutch roll damping and frequency.

Figure 6(d), labeled as "Composite/contour overlay," has the composite contour regions shown as shaded areas, the lighter shade indicating the more desirable region. Superimposed on the same graphic are desirable regions for the control power metric, Mcp, the robustness metric, Mro, and the agility metric, Mag. At this point the final design decision can easily be fine-tuned. Starting at the apparent "best" design point [near $(\zeta, \omega) = (0.4, 1.3)$], the designer may choose to make some important tradeoffs to suit the particular design problem at hand. For example, $\zeta = 0.4$ is at the edge of the desirable region (because it is the edge of Level 1 flying qualities), and it may be more desirable to move the final design point up to a higher damping ratio. As seen in this graphic, the designer has flexibility to move as far up as $\zeta = 0.8$ without substantially reducing the values of the other metrics. This region maintains Level 1 flying qualities, good robustness to model error at the input or output, and relatively low gains. Much less freedom exists for changing the design Dutch roll frequency, however, if the designer is striving for greater agility. In this case, the designer must trade off robustness for agility. For example, moving from approximately $(\zeta, \omega) = (0.4, 1.2)$ to $(\zeta, \omega) = (0.4, 1.6)$ would double the agility metric from 0.1 to 0.2 rad/sec^2, but it would move out of the acceptable robustness region. Since the robustness metric used in this study is very conservative, this may be acceptable. Clearly, the final design requires judgment by the control designer; even more judgment may be required at times, because the best region of an individual metric does not always overlap the other metrics. This complication highlights the nature of control design, which often requires tradeoffs in order to achieve a final overall design. An insightful choice is more readily made using the CRAFT approach because the desirable regions and relative tradeoffs of important metrics are graphically displayed. The designer's choice for a final design of the Dutch roll pole might be chosen with a damping value between 0.4 and 0.6 and a frequency between 1.2 and 1.45 rad/sec. However, the flying qualities specification for Dutch roll damping has not been

developed for high AOA flight. Therefore, in this example, the design choice will be to give up agility for more stability and select a damping and frequency of 0.7 and 1.25 rad/sec, respectively.

Composite Overlay—Final Design—Roll Mode

Using the design selection above for Dutch roll mode, the corresponding roll mode overlay can be developed by performing a CRAFT survey. Figure 7(a) shows the results of evaluating the same design metrics for a roll mode variation. The survey is performed using the same eigenvector design process as for the Dutch roll survey. For this case, the Dutch roll mode is held fixed to the design specified above while the roll mode is allowed to vary from $-4.2\ \text{sec}^{-1}$ to $-0.2\ \text{sec}^{-1}$.

Figure 7(a) shows that increasing control power (Mcp) is required to drive the roll mode to faster values. It reaches its lowest values close to the open-loop roll pole location, $0.2\ \text{sec}^{-1}$. This figure also shows the multivariable robustness metric at the output (Mro) as constant over the range of roll mode considered and therefore it is not a constraint in this design problem. Multivariable robustness at the input (Mri), on the other hand, shows improved or greater values as the roll mode frequency is reduced. Thus, control power demands and robustness are improved as the roll mode is moved to slower values. However, agility degrades with slower placement of the roll mode, as indicated by Mag. The vertical boundary shown in figure 7(a) is a lower limit for the roll mode value as determined from figure 7(b). This particular aircraft achieves maximum stability axis roll rates of 50 deg/sec when operating at 30° AOA. The maximum roll rate is not determined by the inner loop dynamics and therefore must be input to this design process. Various criteria have been used to determine the best roll rate to design into this system, such as the roll overshoot criteria from reference 17. Given 50 deg/sec as a design constraint, the McDonnell Aircraft flying qualities specification from figure 3(a), replotted on figure 7(b), indicates a lower limit for roll mode placement of $-0.8\ \text{sec}^{-1}$. Since this aircraft model is not capable of satisfying design criteria at higher roll rates, the designer is forced into the Level 2 region.

For this design example, the results of the roll mode overlay indicate that a final design choice, with roll mode equal to $-1.4\ \text{sec}^{-1}$ would be satisfactory. With this design choice, desirable levels of robustness are provided, close to minimum gain magnitudes have been obtained (inferring reduced control power required), and at least Level 2 flying qualities have been achieved. This design reflects a choice to trade off maximum roll agility for reduced control power and robustness while respecting flying qualities requirements.

In some cases, further analysis to assess the sensitivity of the roll mode placement on Dutch roll mode overlay might be needed. In this case, however, a repeated CRAFT analysis is not necessary. First, the final roll mode chosen is identical to that used in the Dutch roll mode survey, so there is no change in the Dutch roll survey. Second, additional analysis would not be needed even with a fairly wide range of choices for roll mode since the eigenvectors have been designed to decouple the lateral and directional characteristics. The two surveys are somewhat insensitive to each other because of the decoupled eigenvectors.

The final feedback gains determined using CRAFT for this example provide excellent modal characteristics and decoupling of roll and Dutch roll modes as desired. However, further design is required to obtain a system that gives satisfactory response to pilot inputs. Proper design of feedforward command gains and crossfeeds are also required to obtain a complete, final design ready for pilot commands. Feedforward design is beyond the scope of this paper, but the subject is addressed in reference 26.

Design Issues

Many issues arise for the designer in determining a feedback system for flight. A key concern for the designer using the CRAFT approach with DEA is the determination of a desired eigenspace. This concern is a result of very limited information in the literature on specifying eigenvectors. Fortunately, there is a substantial amount of literature for specifying eigenvalues, although this information is predominantly limited to low AOA. The experience gained in this study designing suitable eigenvectors is discussed in the next section.

One issue that has been removed from the example in this paper, but significantly affects the eigenspace design, concerns redundant control effectors. By using Pseudo Controls in the design model, two independent and orthogonal controls, providing directional and lateral control, replace the conventional redundant controls. The redundant yaw controls are mapped into one independent directional control effector with minimal lateral coupling, and similarly, all the roll control effectors are mapped into an independent lateral control with minimal directional coupling. More details of this approach can be found in reference 25, and details of the application of Pseudo Controls and CRAFT to the HARV control law are found in reference 26. With independent and orthogonal controls, design complexity is greatly simplified, the designer has better insight into the design problem, and implementation costs are significantly reduced. An additional benefit to the designer using DEA is a clear picture of how many elements of the eigenvectors can be exactly specified.

Another issue for the designer, not addressed by this study, is determining the proper set of feedback signals. Although this issue is problem dependent, the choice directly affects the ability of the control system to meet performance specifications. In particular, the choice of feedback measurements and the number of independent feedback measurements directly determine the achievable eigenspace for the closed-loop system. With the DEA approach, each independent feedback measurement allows exact placement of one system eigenvalue. The choice of feedbacks for the example in this paper reflects the constraints of accurate and reliable sensors available for the control law in HARV.

The CRAFT design process provides a mechanism to sort many competing design issues and allow the designer to find desirable placement for the system eigenvalues. However, one issue in the design process involves proper selection of desirable eigenvector characteristics. These characteristics may be constant or variable as the CRAFT survey is performed over the complex plane. Consequently, the designer may require multiple eigenvalue surveys to assess metric sensitivity to design eigenvectors. To demonstrate the sensitivity to eigenvector choice, Mcp is considered for each of the three basic eigenvector design approaches described previously, i.e., open-loop, minimum-specification, and desired-model eigenvectors. Mcp defines RMS gain magnitude that reflects demands on the control system to change system dynamics from existing open-loop characteristics to desired closed-loop characteristics. The more demanding changes in terms of eigenvalues or eigenvectors are reflected in the greater magnitude of this metric.

System scaling is an issue that arises when using DEA and CRAFT, because it can help with interpretation of the eigenvectors in the design process. System scaling, however, was not used in this study because Psuedo Controls attempt to provide a unity transfer function to the feedbacks. Only scaling for final presentation of eigenvectors is used in this report, as noted previously. From a control designer's point of view it is important to note that scaling the system, implemented as a similarity transform, affects the eigenvectors and gains that result from the design process. Therefore, interpretation of gains and eigenvectors must be done with knowledge of any scaling. However, the system responses and eigenvalues are independent of similarity transforms on the system.

To demonstrate the impact of eigenvector choice on design, the current work performs analysis with four different eigenvector specifications. For each case the control power metric, Mcp, is considered as a function of Dutch roll mode frequency and damping. In all four cases, eigenvector design choices have been applied to the 30° AOA model for calculating feedback gains and to the Mcp metric. The first two cases considered utilize open-loop eigenvectors that remain constant as the Dutch roll mode pole is varied. These two cases utilize open-loop eigenvectors that are taken from 5° and 30° AOA models, respectively. The third and fourth cases utilize minimum-specification and desired-model eigenvectors. For these eigenvector choices, the eigenvector specification varies with choice of Dutch roll mode pole.

Open-Loop Eigenvectors

The first approach for eigenvector design considered in this study was the use of the open-loop eigenvectors of the system. As described earlier, this approach works well with an aircraft that behaves classically already but may need some adjustments to its eigenvalues. The resulting eigenspace for the 30° AOA design point, using 5° AOA open-loop eigenvectors as desired eigenvectors, is shown in table 4. Transformation of side velocity, v, to sideslip, β, has not been done for these eigenspace comparisons, so comparisons of desired and achieved eigenvectors, as well as the impact of eigenvector choice on RMS gains (Mcp), can be made directly.

Table 4. Design Closed-Loop Eigenspace at 30° AOA
Using 5° AOA Open-Loop Eigenvectors

State	Dutch roll mode	Roll mode	Spiral mode
Final Design: Closed-Loop Eigenvalues			
	$-0.8750 \pm 0.8927j$	−1.40	−0.050
Final Design: Desired Closed-Loop Eigenvectors			
v	(1.0, 0.0)†	1.0	1.0
p_{stab}	(0.0087, 134.0)	−0.1133	0.0027
r_{stab}	(0.0026, 277.69)	0.0064	0.0337
ϕ_{stab}	(0.0052, 36.87)	0.0809	0.6312
Final Design: Achieved Closed-Loop Eigenvectors			
v	(1.0, 0.0)	1.0	1.0
p_{stab}	(0.0064, −188.12)	−0.1133	−0.0295
r_{stab}	(0.0044, −40.15)	0.0122	0.0718
ϕ_{stab}	(0.0052, 36.87)	0.0811	0.6312

†(magnitude, phase [deg])

The final design eigenvalues are exactly as desired, since there are four independent measurements in this design problem. However, with only two independent controls, only two elements of each eigenvector could be specified. The final achieved eigenvectors match the desired eigenvectors for those elements that were weighted. For example, the first and last elements of the Dutch roll eigenvectors, the first and second elements of the roll mode eigenvector, and the first and last elements of the spiral mode eigenvector were weighted. Consequently, for these elements the achieved values match desired values exactly.

The resulting eigenspace at the final design point, using 30° AOA open-loop eigenvectors as desired eigenvectors, is given in table 5. Again the desired and achieved values of the eigenspace match where weights were applied in the DEA algorithm to force the match. As in the previous case, the unweighted

elements of the eigenvectors are allowed to vary in order to match, in a least squares sense, an achievable eigenspace to the desired eigenspace. Considering the achieved eigenvectors from the two designs using open-loop eigenvectors, one cannot easily discern the impact on the final design. Using design metrics such as Mcp can provide more insight, because the final design is sensitive to these measures, and these measures are important to the designer.

The impact on Mcp of choosing an open-loop eigenvector specification is shown in figures 8(a) and 8(b). These eigenvector specifications are constant as Dutch roll mode frequency and damping are varied during the CRAFT survey. Figure 8(a) shows the impact of choosing desired eigenvectors from a 5° AOA, open-loop model and figure 8(b) shows the results of choosing from a 30° AOA, open-loop model. Comparing these two cases, the more classical eigenvector from the lower AOA model produced the lower values of RMS feedback gains overall, and it produced the largest region of low Mcp values, i.e., values of Mcp ≤ 2. This makes the designer's work easier, giving more freedom of choice for the final pole placement. Both cases show regions of lower metric values near Dutch roll mode frequencies of 1 rad/sec; however, the shapes of the low valued regions and nearby gradients are substantially different. Figures 8(a) and 8(b) highlight the sensitivity of the final design to choice of desired eigenvectors.

Table 5. Design Closed-Loop Eigenspace at 30° AOA
Using 30° AOA Eigenvectors

State	Dutch roll mode	Roll mode	Spiral mode
Final Design: Closed-Loop Eigenvalues			
not applicable	$-0.8750 \pm 0.8927j$	−1.40	−0.050
Final Design: Desired Closed-Loop Eigenvectors			
v	(1.0, 0.0)†	1.0	1.0
p_{stab}	(0.0075, 112.96)	−0.0151	−0.0048
r_{stab}	(0.0046, 292.98)	0.0091	0.0106
ϕ_{stab}	(0.0061, 6.93)	0.0751	0.0927
Final Design: Achieved Closed-Loop Eigenvectors			
v	(1.0, 0.0)	1.0	1.0
p_{stab}	(0.0075, −218.62)	−0.0151	−0.0043
r_{stab}	(0.0048, −40.28)	0.0060	0.0106
ϕ_{stab}	(0.0061, 6.93)	0.0109	0.0927

†(magnitude, phase [deg])

In general, as a CRAFT survey moves the values of the target closed-loop poles toward the open-loop poles, while using the system open-loop eigenvectors, the gains will go to zero. However, the design using 30° AOA, open-loop eigenvectors [shown in figure 8(b)] did not produce a large area of reduced Mcp, and the gains did not go to zero near the open-loop pole locations. In this case, the lower gains are not achieved because the 30° AOA eigenvectors are used in combination with eigenvalues that are not all selected close to their open-loop values. For this design example, the desired closed-loop roll mode is substantially different from the system's open-loop value; consequently, the final design has an eigenspace different from an open-loop eigenspace that would have produced reduced feedback gains. Feedback gain magnitudes generally reflect the degree of difference between open-loop and desired closed-loop eigenspace.

Eigenvector choice has a significant impact on feedback gains. Unfortunately, there is not much guidance available for determining the best eigenvectors. The open-loop eigenvector may be a valid

choice if the open-loop airframe has been designed to provide classical airframe dynamics. This strategy can be successful at low AOA, but it does not necessarily give the best dynamics over a full range of AOA. In addition, it is not likely to give the best dynamics when forcing open-loop eigenvectors to match with design eigenvalues that are significantly different from the open-loop eigenvalues. Mathematically, eigenvectors must match the real or complex nature of the corresponding eigenvalues. A constant eigenvector may violate this constraint when, for example, Dutch roll damping is high, leading to two real poles instead of a complex pair. In either case the feedback gains tend to become large quickly as the design pole moves away from the open-loop position. These difficulties can be reduced or removed by adjustments in the eigenvectors that reflect both the desires of the designer and the physical and mathematical relationships that connect eigenvalues and eigenvectors. Some adjustments that are useful are discussed in the next two sections.

Minimum-Specification Eigenvectors

As discussed previously, this approach is the most straightforward method to obtain eigenvectors. The designer simply specifies each element of the eigenvector to be 0 or 1, as appropriate, to achieve desired decoupling of the aircraft rigid body modes. This method is facilitated by using DEA that finds the closest achievable eigenvector to the "desired" eigenvector. This method has been used with success in application to the HARV lateral-directional control law design (refs. 26, 27). The HARV design and the example in this paper were done using an optimization procedure to provide appropriate ϕ/β ratio over the CRAFT design space and to minimize gain magnitudes.

The desired and achieved eigenspace at the final design point is given in table 6. As for the previous open-loop eigenvector design case, the states, $X = [v\ p_{stab}\ r_{stab}\ \phi_{stab}]$, have not been scaled. Unlike the open-loop eigenvectors, the minimum-specification eigenvectors allow the first elements of the roll and spiral modes to be specified exactly as zero. Consequently, for presentation of these eigenvectors, the last element is used to normalize the vector.

Table 6. Design Closed-Loop Eigenspace at 30° AOA
Using Minimum-Specification Eigenvector

State	Dutch roll mode	Roll mode	Spiral mode
Final Design: Closed-Loop Eigenvalues			
not applicable	–0.8750 + 0.8927j	–1.40	–0.050
Final Design: Desired Closed-Loop Eigenvectors			
v	(1.0, 0.0)†	0.0	0.0
p_{stab}	(x.x, x.x)	1.0	x.x
r_{stab}	(x.x, x.x)	x.x	x.x
ϕ_{stab}	(0.0065, 0.0)	x.x	1.0
Final Design: Achieved Closed-Loop Eigenvectors			
v	(1.0, 0.0)	0.0	0.0
p_{stab}	(0.0080, 134.34)	–1.3975	–0.0468
r_{stab}	(0.0049, –40.43)	0.0879	0.1138
ϕ_{stab}	(0.0065, 0.0)	1.0	1.0

†(magnitude, phase [deg])

Figure 8(c) shows the results of using the minimum-specification eigenvector approach in the example problem. Contours of Mcp are shown for the CRAFT survey of Dutch roll frequency and damping. A

fairly large area in the design space below a Dutch roll frequency of 1.5 rad/sec has very low feedback gains. A fairly sharp increase of Mcp occurs with this approach for frequencies between 1.5 and 1.6 rad/sec; above 1.6 rad/sec, the magnitude of Mcp levels out to values slightly under that found with the 30° AOA open-loop eigenvector. This rapid change in gains reflects the sensitivity of feedback gains to eigenvectors. Part of this sensitivity is due to a limit on allowable ϕ/β ratios, which was reached during the optimization to minimize RMS gain magnitude.

This sensitivity also reflects the need for caution when specifying eigenvectors in a minimum-specification manner. Eigenvectors can be specified directly as linearly independent combinations of zeroes and ones, as is often seen in the literature when eigenspace assignment is used. It provides a direct way to decouple responses of aircraft states. However, this neither respects physical constraints of the aircraft nor modal requirements that may exist. The choice of eigenvalue and eigenvector is closely related to specifying the placement of poles and zeroes in a transfer function representation. Transfer function zeroes are functions of aircraft physical characteristics; for example, $T_{\theta 2}$ is directly tied to $C_{L\alpha}$. Consequently, specifying nonaircraft-like values for these parameters may result in physically unachievable eigenvectors and large gains. Fortunately, eigenspace assignment allows a solution for the achievable eigenvectors that are as close to the desired eigenspace as possible, but there is no guarantee of small gains at the solution point. Very high gains imply the theoretically achievable eigenspace is not practical. The designer must work a tradeoff between desirable eigenspace and available control power.

Desired-Model Eigenvectors

Creating desired-model eigenvectors by first creating a state-space model that expresses the eigenspace explicitly is an approach that has also been used with success. This method, although not as simple as the minimum-specification method, is straightforward. It does, however, require more a priori information to create the desired state-space model. This additional information for the desired model may not be available in some cases, for example, at high AOA conditions where there is limited design experience.

Figure 8(d) shows the contours of Mcp for this choice of eigenvector design. This method produced the lowest values of Mcp of all the approaches considered, reinforcing the idea that the RMS gains are kept lowest with eigenvector designs that vary during the CRAFT survey. For the example, in the 30° AOA system in this paper, the desired-model approach provided a larger region of acceptable values for Mcp than the minimum-specification approach. This result highlights the sensitivity of eigenvector choice because the resultant eigenvectors at the final design point are very similar between the two methods. Table 7 shows the final design eigenspace resulting from design with desired-model eigenvectors. The achieved eigenspace using desired-model eigenvectors appears very close to that achieved using minimum-specification eigenvectors; however, it is clear from figure 8 that potentially large differences exist from a control designer's point of view. These differences highlight the sensitivity of the control designer's problem to eigenspace choice and the need for a CRAFT design methodology.

Table 7. Design Closed-Loop Eigenspace at 30° AOA
Using Desired-Model Eigenvectors

State	Dutch roll mode	Roll mode	Spiral mode
Final Design: Closed-Loop Eigenvalues			
not applicable	–0.8750 + 0.8927j	–1.40	–0.050
Final Design: Desired Closed-Loop Eigenvectors			
v	(1.0, 0.0)†	0.0	0.0
p_{stab}	(0.0095, 120.46)	0.8036	0.0
r_{stab}	(0.0032, –90.0)	0.0	0.0
ϕ_{stab}	(0.0078, –12.28)	–0.5952	1.0
Final Design: Achieved Closed-Loop Eigenvectors			
v	(1.0, 0.0)	0.0	0.0
p_{stab}	(0.0097, 121.89)	–1.3975	–0.0468
r_{stab}	(0.0051, –40.69)	0.0879	0.1138
ϕ_{stab}	(0.0078, –12.28)	1.0	1.0

†(magnitude, phase [deg])

Concluding Remarks

A control law design method known as CRAFT has been introduced to provide greater insight into control law design tradeoffs by using a combination of Direct Eigenspace Assignment and a graphical approach for representing control law design metrics. CRAFT promotes efficient integration of multiple design goals. Any quantifiable design goal sensitive to the closed-loop dynamics can be included as a metric in this design process. The method allows the designer to use a building block approach to select or emphasize a particular required capability and at the same time achieve a balanced overall design integrating many diverse requirements. In particular, it fosters selection of dynamics that provide the greatest agility available while satisfying appropriate levels of flying qualities, controlling system robustness, and respecting the available control power. The approach allows multi-input, multi-output design without requiring full-state feedback, and by control of the closed-loop eigenspace, flying qualities specifications can be incorporated into the design.

The CRAFT methodology provides insights into tradeoffs for some common difficulties associated with eigenspace assignment, such as large gains and a lack of robustness guarantees. These insights are provided through graphical display of the desirable regions for robustness and gain magnitudes. In addition, the sensitivity of metrics to pole placement is clearly displayed, providing an indicator of the best directions to move poles for improvement. Engineering judgment is required by the user, however, to specify the dynamics (in particular, eigenvectors) with appropriate values to ensure acceptable gain magnitudes. In the final analysis, the CRAFT overlay plot enables the designer to tailor the final design by selecting acceptable levels for a variety of metrics or to emphasize particular design goals. As technology develops and experience is gained with advanced fighter designs, CRAFT may be used for developing new metrics and refining existing metrics to provide greater sensitivity to design tradeoffs.

References

1. Herbst, W. B.; and Krogull, B.: Design for Air Combat. AIAA 72-749, Aug. 1972.

2. Eidetics International, Inc: *Tactical Evaluation of the Air-to-Air Combat Effectiveness of Supermaneuverability*. WRDC-TR-90-3035, June 1990.

3. McDonnell Aircraft Co., McDonnell Douglas Corp: *Multi-System Integrated Control (MuSIC) Program*. WRDC-TR-90-6001, June 1990.

4. Herbst, W.: Future Fighter Technologies. *J. Airc*., vol. 17, no. 8, Aug. 1980.

5. Hamilton, W. L.; and Skow, A. M.: *Operational Utility Survey: Supermaneuverability*. AFWAL-TR-85-3020, Sept. 1984.

6. Ogburn, M. E.; Nguyen, L. T.; Wunschel, A. J.; Brown, P. W.; Carzoo, S. W.: *Simulation Study of Flight Dynamics of a Fighter Configuration With Thrust-Vectoring Controls at Low Speeds and High Angles of Attack*. NASA TP-2750, 1988.

7. Foltyn, Robert W.; Skow, Andrew W.; Lynch, Urban H.; Lynch, Anerew M. P.; Laboy, Orlando J.; Arand, Anthony J.: *Development of Innovative Air Combat Measures of Merit for Supermaneuverable Fighters.* AFWAL-TR-87-3073, Eidetics, Oct. 1987.

8. Hodgkinson, J.; Skow, A.; Ettinger, R.; Lynch, U.; Laboy, O.; Chody, J.; Cord, T. J.: Relationships Between Flying Qualities, Transient Agility, and Operational Effectiveness of Fighter Aircraft. AIAA 88-4327, Aug. 1988.

9. Phillips, William H.: *Analysis of Effects of Interceptor Roll Performance and Maneuverability on Success of Collision-Course Attacks*. NACA RM L58E27, 1958.

10. McAtee, Thomas P.: Agility in Demand. *Aerosp. America*, May 1988.

11. Tamrat, B. F.: Fighter Aircraft Agility Assessment Concepts and Their Implication on Future Agile Fighter Design. AIAA 88-4400, Sept. 1988.

12. Skow, Andrew M.; Hamilton, William L.; Taylor, John H.: Advanced Fighter Agility Metrics. AIAA 85-1779, Aug. 1985.

13. Taylor, John H.; Skow, Andrew M.; Parker, Robert W.; Malcolm, Gerald N.; Folytn, Robert W.: *Flight Test Validation of Advanced Agility Metrics for T-38 and F-4*. USAF Contract F33615-85-C-0120, TR 86-212, Sept. 1986.

14. Skow, Andrew M.; Foltyn, Robert W.; Taylor, John H.; Parker, Robert W.: *Transient Performance and Maneuverability Measures of Merit for Fighter/Attack Aircraft*. USAF Contract F33615-85-C-0120, TR 86-201, Jan. 1986.

15. Murphy, P. C.; Bailey, M. L.; and Ostroff, A. J: *Candidate Control Design Metrics for an Agile Fighter*. NASA TM-4238, 1991.

16. Foster, J. V.; Bundick, W. T.; and Pahle, J. W.: *Controls for Agility Research in the NASA High-Alpha Technology Program*. SAE TP-912148, Sept. 1991.

17. Hoffler, K. D.; Brown, P. W.; Phillips, M. R.; Rivers, R. A.; Davidson, J. B.; Lallman, F. J.; Murphy, P. C.; and

Ostroff, A. J.: Evaluation Maneuver and Guideline Development for High-Alpha Control Law Design Using Piloted Simulation. AIAA 94-3512, Aug. 1994.

18. Wilson, D. J.; and Riley, D. R.: *Volume 1 and 2: Flying Qualities Criteria Development Through Manned Simulation for 60° Angle-of-Attack*. NASA CR-4535, 1993.

19. Chambers, Joseph R.; Gilbert, William P.; Nguyen, Luat T., eds.: *High-Angle-of-Attack Technology*. NASA CP-3149, 1990.

20. Matheny, N. W., compiler: *High-Angle-of-Attack Projects and Technology Conference*. NASA CP-3137, 1992.

21. *Fourth High Alpha Conference*. NASA CP-10143, 1994.

22. *Fifth High Alpha Conference*. NASA/CP-1998-207676, 1998.

23. Nguyen, Luat T.: *Flight Dynamics Research for Highly Agile Aircraft*. SAE TP-892235, Sept. 1989.

24. Murphy, P. C.; and Davidson, J. B.: Control Design for Future Agile Fighters. AIAA 91-2882, Aug. 1991.

25. Lallman, F. J.; Davidson, J. B.; and Murphy, P. C.: *A Method for Integrating Thrust-Vectoring and Actuated Forebody Strakes With Conventional Aerodynamic Controls on a High-Performance Fighter Airplane*. NASA/TP-1998-208464, 1998.

26. Davidson, J. B.; Murphy, P. C.; Lallman, F. J.; Hoffler, K. D.; and Bacon, B. J.*: High-Alpha Research Vehicle Lateral-Directional Control Law Description, Analyses, and Simulation Results.* NASA/TP-1998-208465, 1998.

27. HARV Control Law Design Team: *Design Specification for a Thrust-Vectoring, Actuated-Nose-Strake Flight Control Law for the High-Alpha Research Vehicle*. NASA TM-110217, 1996.

28. Davidson, J. B.; and Schmidt, D. K.: *Flight Control Synthesis for Flexible Aircraft Using Eigenspace Assignment*. NASA CR-178164, 1986.

29. Srinathkumar, S.: *Modal Control Theory and Application to Aircraft Lateral Handling Qualities Design*. NASA TP-1234, 1978.

30. *Military Standard—Flying Qualities of Piloted Aircraft*. MIL-STD-1797A, Jan. 1990.

31. Shapiro, E. Y.; and Chung, J. C.: Flight Control System Synthesis Using Eigenstructure Assignment. *J. Optim. Theory & Appl*., vol. 43, no. 3, July 1984.

32. Farineau, J.: Lateral Electric Flight Control Laws of a Civil Aircraft Based Upon Eigenstructure Assignment Technique. AIAA 89-3594, Aug. 1989.

33. Unbehauen, H.; and Rao, G. P.: *Identification of Continuous Systems, North-Holland Systems and Control Series*. Elsevier Sci. Publ. Co., Inc., 1987.

34. Mukhopadhyay, V.; and Newsom, J. R.: A Multiloop System Stability Margin Study Using Matrix Singular Values. *J. Guid., Navigat., & Control*, vol. 8, no. 4, Sept.–Oct. 1984.

35. Bitten, R.: Qualitative and Quantitative Comparison of Government and Industry Agility Metrics. AIAA-89-3389-CP, Aug. 1989.

36. Moorhouse, D. J.; and Moran, W. A.: Flying Qualities Design Criteria for Highly Augmented Systems. *IEEE National Aerospace and Electronics Conference*, NAECON, May 1985.

37. Riley, David R.; and Drajeske, Mark H.: Relationships Between Agility Metrics and Flying Qualities. *SAE Aerospace Atlantic Conference*, SAE TP-901003, April 1990.

38. Krekeler, Gregory C.; Wilson, David J.; and Riley, David R.: High Angle-of-Attack Flying Qualities Criteria. AIAA 90-0219, Jan. 1990.

39. Neal, P. T.; and Smith, R. E.: *An In-Flight Investigation to Develop Control System Design Criteria for Fighter Airplanes.* AFFDL-TR-70-74, vol. 1, Dec. 1970.

40. Smith, R.; and Geddes, N. D.: *Handling Quality Requirements for Advanced Aircraft Design: Longitudinal Mode*. AFFDL-TR-78-154, Aug. 1979.

41. Gibson, J. C.: *Piloted Handling Qualities Design Criteria for High Order Flight Control Systems*. AGARD-CP-333, 1982.

Appendix

Open-loop system quadruples, describing 4th order, linear, lateral-directional dynamics of HARV with thrust-vectoring at 5° and 30° AOA, are shown below. System quadruples have the form of

$$\text{Sys\_AOA} = \begin{bmatrix} A & B \\ M & N \end{bmatrix}$$

which define state-space equations for states, X, controls, U, and measurements, Z, as

$$\dot{X} = AX + BU$$
$$Z = MX + NU$$

System states are side velocity (ft/sec), stability-axis roll rate (rad/sec), stability-axis yaw rate (rad/sec), and stability-axis bank angle (rad). Two Pseudo Control inputs are normalized pseudo lateral control and normalized pseudo yaw control. Measurements for feedback are stability-axis roll rate, stability-axis yaw rate, lateral acceleration at the sensor (g's), and sideslip rate (rad/sec). Trim values for total velocities are 598.0 ft/sec at 5° AOA and 282.0 ft/sec at 30° AOA.

Sys_05 =

–0.1305	0.1512	–597.5821	32.1667	–2.0005	–19.1022
–0.0187	–1.5271	0.6757	0.0	1.1179	–0.1941
0.0050	0.1152	–0.1529	0.0	0.0096	1.3527
0.0	1.0	0.0	0.0	0.0	0.0
0.0	1.0	0.0	0.0	0.0	0.0
0.0	0.0	1.0	0.0	0.0	0.0
–0.0021	0.0535	–0.0462	0.0	–0.0614	–0.0669
–0.0002	0.0003	–0.9992	0.0538	–0.0033	–0.0319

Sys_30 =

–0.0403	–0.1337	–282.2581	32.1549	–4.5212	–8.6376
–0.0099	–0.3858	0.7811	0.0	0.6768	–0.2130
0.0060	0.2001	–0.5262	0.0	0.1948	1.1910
0.0	1.0	–0.0280	0.0	0.0	0.0
0.0	1.0	0.0	0.0	0.0	0.0
0.0	0.0	1.0	0.0	0.0	0.0
–0.0007	0.0041	–0.0675	0.0	–0.0145	0.0296
–0.0001	–0.0005	–1.0009	0.1140	–0.0160	–0.0306

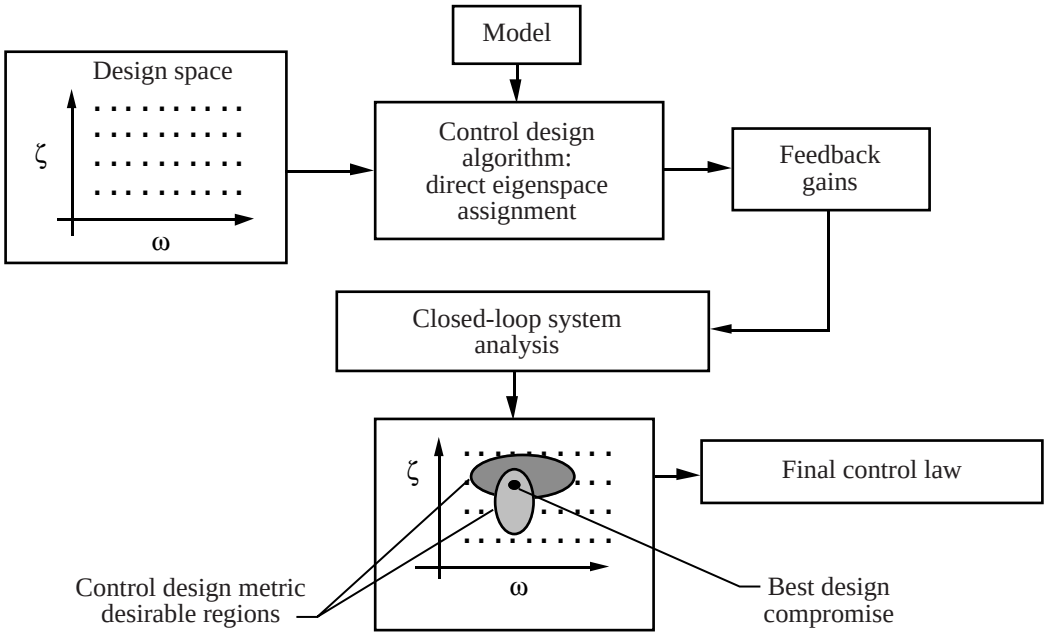

Figure 1. CRAFT control synthesis methodology.

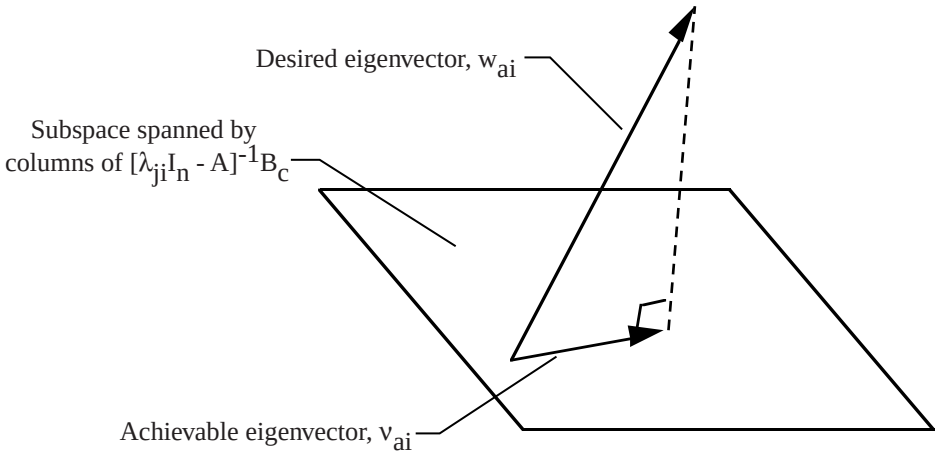

Figure 2. Achievable eigenvector obtained through DEA.

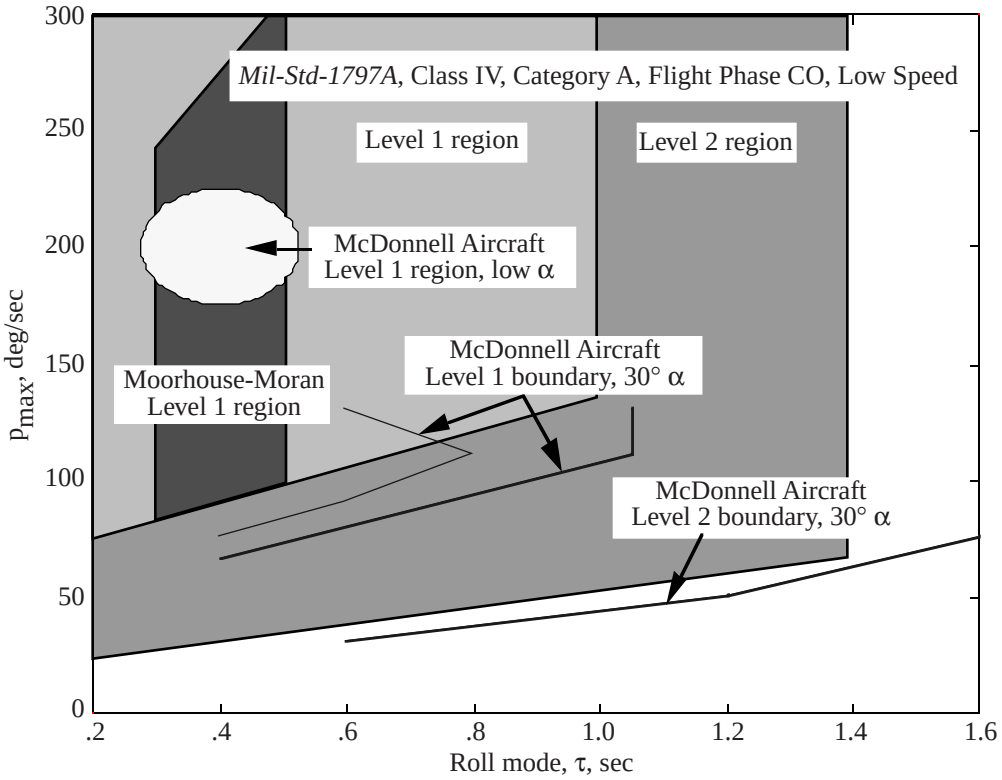

(a) Gross acquisition flying qualities levels.

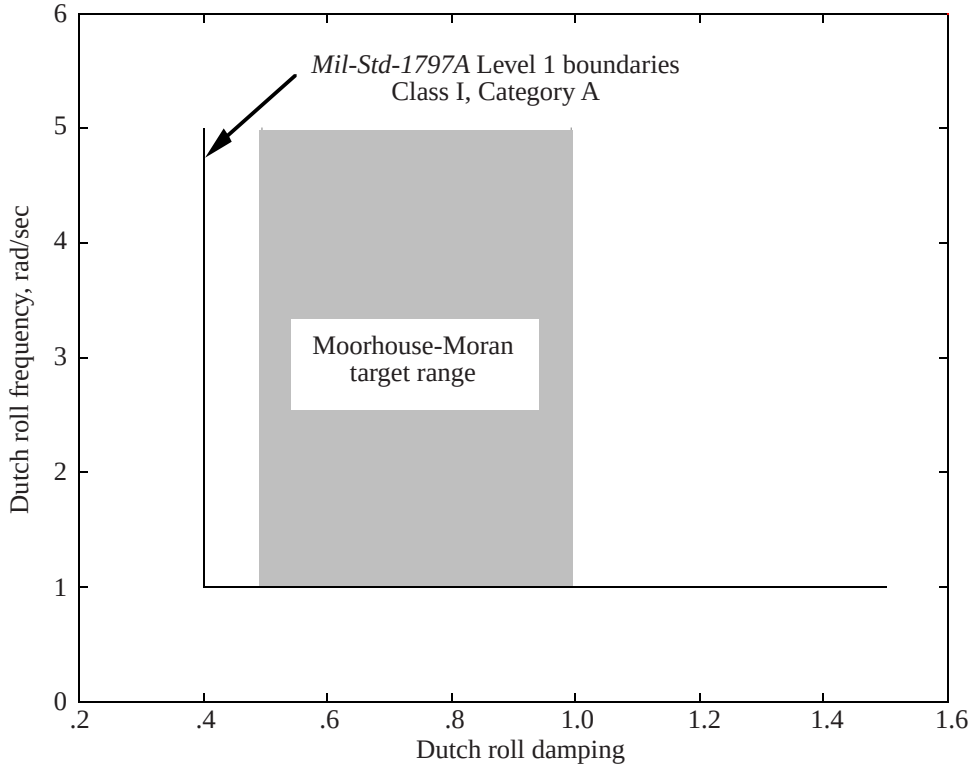

(b) Low alpha Dutch roll flying qualities criteria.

Figure 3. Flying qualities criteria.

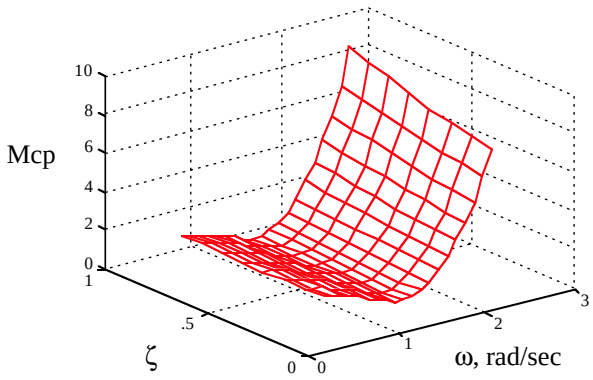

(a) Control power, Mcp

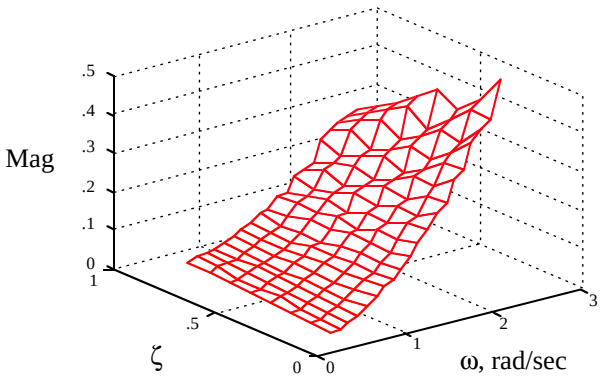

(b) Agility, Mag

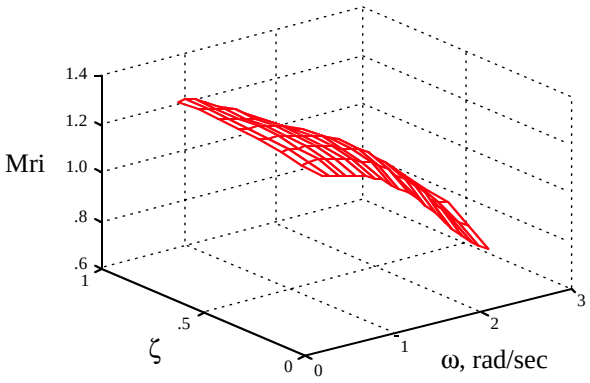

(c) Input robustness, Mri

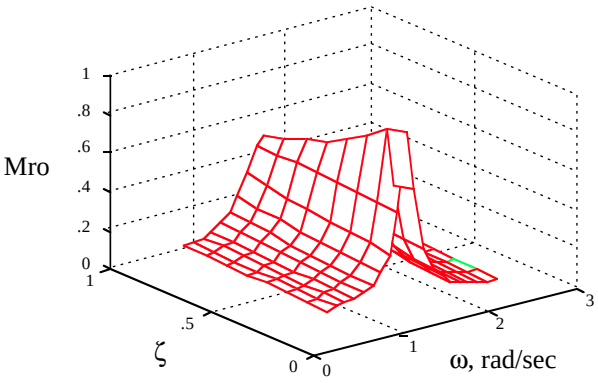

(d) Output robustness, Mro

Figure 4. CRAFT metrics for Dutch roll mode variation.

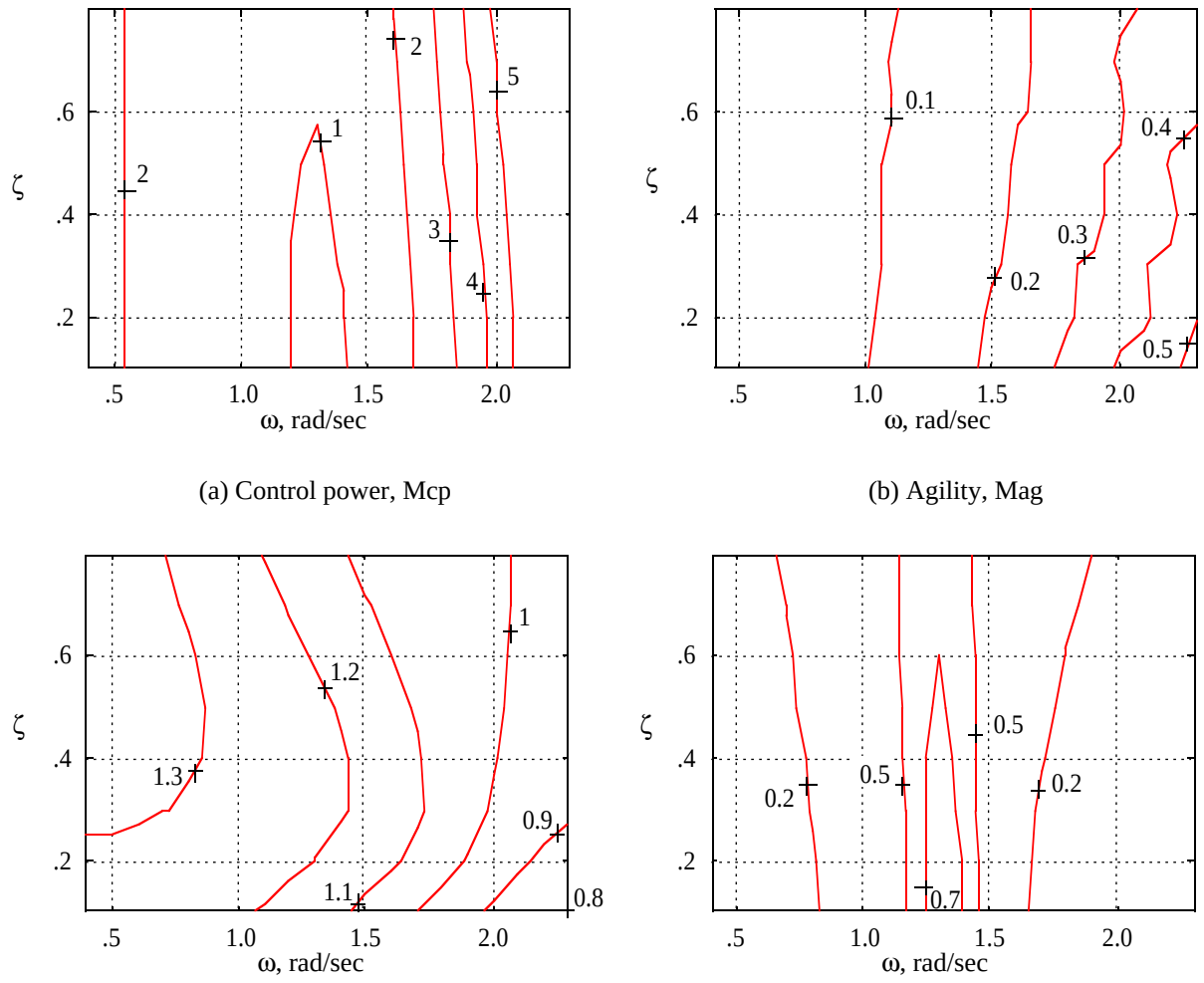

(a) Control power, Mcp

(b) Agility, Mag

(c) Input robustness, Mri

(d) Output robustness, Mro

Figure 5. CRAFT metrics for Dutch roll mode variation.

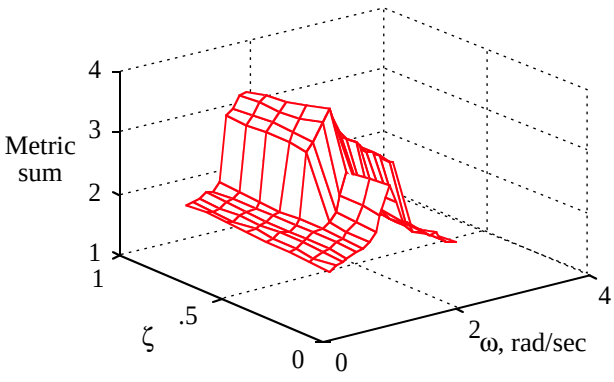

(a) Composite metric surface

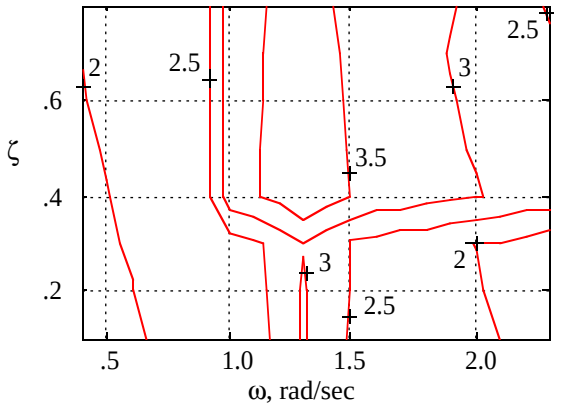

(b) Composite metric contours

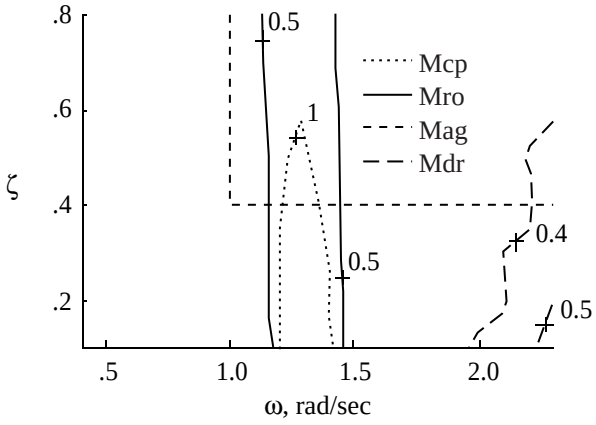

(c) Metric desired regions

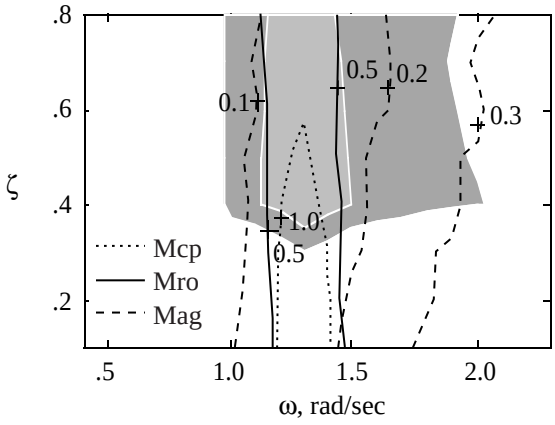

(d) Composite/contour overlay

Figure 6. Metric composite, desired contours, and final overlay.

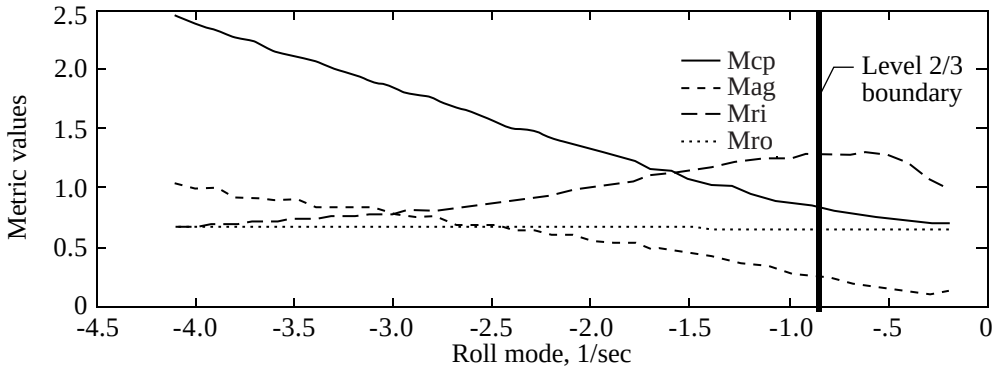

(a) CRAFT overlay for roll mode survey

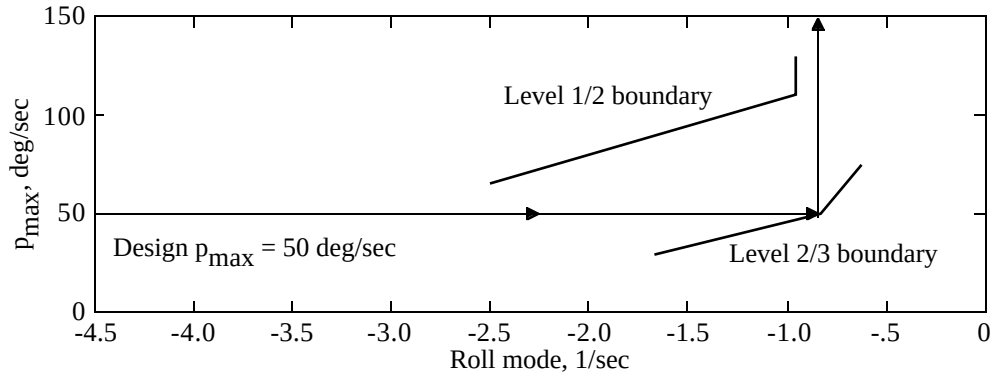

(b) CRAFT overlay for roll mode survey

Figure 7. Roll mode requirements for gross acquisition.

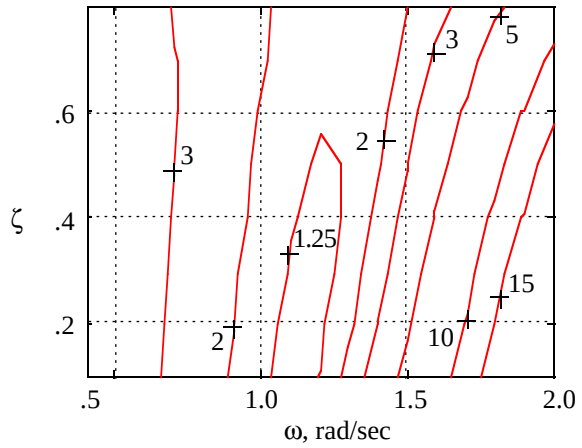

(a) Constant open-loop eigenvector 5° AOA

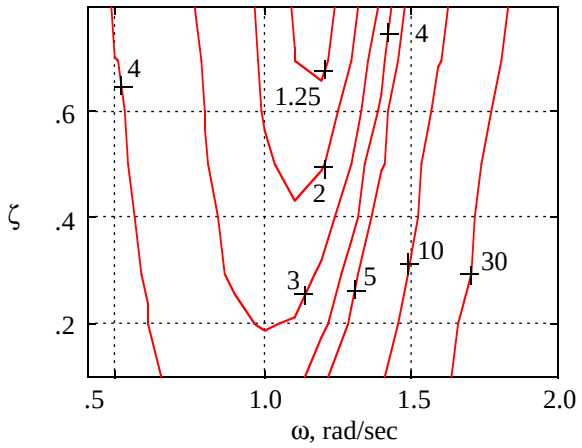

(b) Constant open-loop eigenvector 30° AOA

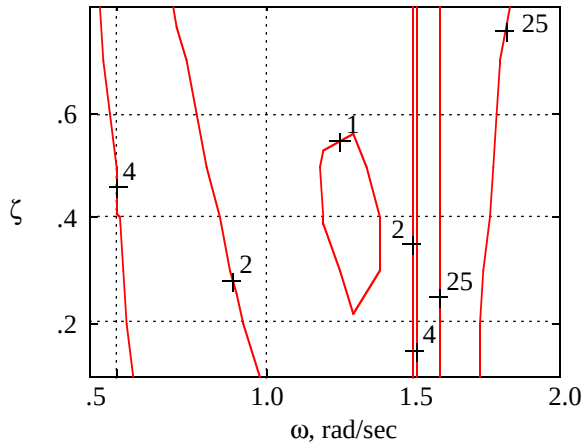

(c) Minimum-specification eigenvector

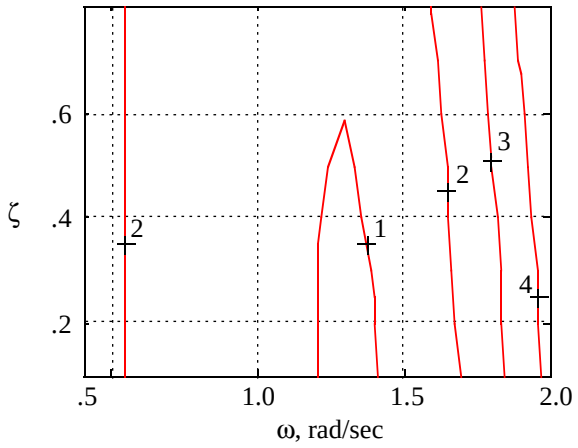

(d) Desired-model eigenvector

Figure 8. Variation of control power metric, Mcp, with eigenvector selection.

REPORT DOCUMENTATION PAGE

Form Approved
OMB No. 07704-0188

Public reporting burden for this collection of information is estimated to average 1 hour per response, including the time for reviewing instructions, searching existing data sources, gathering and maintaining the data needed, and completing and reviewing the collection of information. Send comments regarding this burden estimate or any other aspect of this collection of information, including suggestions for reducing this burden, to Washington Headquarters Services, Directorate for Information Operations and Reports, 1215 Jefferson Davis Highway, Suite 1204, Arlington, VA 22202-4302, and to the Office of Management and Budget, Paperwork Reduction Project (0704-0188), Washington, DC 20503.

1. AGENCY USE ONLY *(Leave blank)*	2. REPORT DATE	3. REPORT TYPE AND DATES COVERED
	September 1998	Technical Publication

4. TITLE AND SUBTITLE
A Control Law Design Method Facilitating Control Power, Robustness, Agility, and Flying Qualities Tradeoffs: CRAFT

5. FUNDING NUMBERS
WU 505-68-30-05

6. AUTHOR(S)
Patrick C. Murphy and John B. Davidson

7. PERFORMING ORGANIZATION NAME(S) AND ADDRESS(ES)
NASA Langley Research Center
Hampton, VA 23681-2199

8. PERFORMING ORGANIZATION REPORT NUMBER
L-17571

9. SPONSORING/MONITORING AGENCY NAME(S) AND ADDRESS(ES)
National Aeronautics and Space Administration
Washington, DC 20546-0001

10. SPONSORING/MONITORING AGENCY REPORT NUMBER
NASA/TP-1998-208463

11. SUPPLEMENTARY NOTES

12a. DISTRIBUTION/AVAILABILITY STATEMENT
Unclassified–Unlimited
Subject Category 08 Distribution: Standard
Availability: NASA CASI (301) 621-0390

12b. DISTRIBUTION CODE

13. ABSTRACT *(Maximum 200 words)*

A multi-input, multi-output control law design methodology, named “CRAFT”, is presented. CRAFT stands for the design objectives addressed, namely, Control power, Robustness, Agility, and Flying Qualities Tradeoffs. The methodology makes use of control law design metrics from each of the four design objective areas. It combines eigenspace assignment, which allows for direct specification of eigenvalues and eigenvectors, with a graphical approach for representing the metrics that captures numerous design goals in one composite illustration. Sensitivity of the metrics to eigenspace choice is clearly displayed, enabling the designer to assess the cost of design tradeoffs. This approach enhances the designer’s ability to make informed design tradeoffs and to reach effective final designs. An example of the CRAFT methodology applied to an advanced experimental fighter and discussion of associated design issues are provided.

14. SUBJECT TERMS	15. NUMBER OF PAGES
Control law design; Design tradeoffs; Feedback control; Feedback gains; Output feedback; Eigenspace assignment; High performance aircraft; High angle of attack; Fighter aircraft; Metrics; Agility; Robustness; Flying qualities; Handling qualities	45
	16. PRICE CODE A03

17. SECURITY CLASSIFICATION OF REPORT	18. SECURITY CLASSIFICATION OF THIS PAGE	19. SECURITY CLASSIFICATION OF ABSTRACT	20. LIMITATION OF ABSTRACT
Unclassified	Unclassified	Unclassified	